# Desalination of Brackish Groundwater in the United States: Minimum Energy Requirements

by

Yvana D. Ahdab

B.S., Johns Hopkins University (2015)

Submitted to the Department of Mechanical Engineering
in partial fulfillment of the requirements for the degree of

Master of Science in Mechanical Engineering

at the

MASSACHUSETTS INSTITUTE OF TECHNOLOGY

June 2017



Signature redacted

Author .....
Department of Mechanical Engineering
May 12, 2017

Signature redacted

Certified by .....
John H. Lienhard V
Abdul Latif Jameel Professor of Water
Thesis Supervisor

Signature redacted

Accepted by .....
Rohan Abeyaratne
Chairman, Committee on Graduate Students

# Desalination of Brackish Groundwater in the United States: Minimum Energy Requirements

by

Yvana D. Ahdab

Submitted to the Department of Mechanical Engineering
on May 12, 2017, in partial fulfillment of the
requirements for the degree of
Master of Science in Mechanical Engineering

## Abstract

Water scarcity around the globe has motivated rising interest in desalinating brackish groundwater to meet fresh water demand. Various organizations in the United States have collected more hydrological and chemical data from the growing number of wells. Yet, only one national assessment of groundwater resource distribution and availability has been conducted in the United States since the 1960s, and no national assessment has been conducted on the energy costs required to make brackish groundwater potable. Because the ionic composition of groundwater varies significantly from location to location, unlike seawater, conducting site-specific analyses of the resource across the U.S. is necessary. This thesis uses chemical and physical data from a U.S. Geological Survey dataset compiled in 2017, including samples from over 100,000 groundwater wells across the United States, to carry out a nationwide investigation of brackish groundwater composition and minimum desalination energy costs. Beginning with a full Pitzer-Kim mixed electrolyte model, we develop a thermodynamic analysis of the least work of separation in order to compute the site-specific least work of separation required for groundwater desalination. Least work of separation represents a baseline for specific energy consumption of real-world desalination systems. Then, we study the geographic distribution of least work of separation to determine areas with both low least work of separation and high water stress. These regions hold potential for desalination to decrease the disparity between high water demand and low water supply. We develop simplified equations for least work as a function of recovery ratio and the following parameters: total dissolved solids, specific conductance, ionic strength, and molality. Lastly, we examine the effects of groundwater composition on minimum energy costs, and the geographic distribution of total dissolved solids, well depth and major ions.

Thesis Supervisor: John H. Lienhard V
Title: Abdul Latif Jameel Professor of Water

# Acknowledgments

My deepest gratitude is extended to my advisor, Professor John Lienhard. His guidance, technical expertise, and support have been invaluable. I would like to thank my former lab mate, Gregory P. Thiel, for his crucial contributions to this work. Acknowledgment is also given to my lab mates and friends in the Lienhard Research Group for valuable discussions and advice.

I would also like to thank the U.S. Geological Survey for providing the dataset necessary to carry out the analyses in this thesis and to the Center for Clean Water Energy at MIT and the King Fahd University of Petroleum and Minerals for funding the research reported in this thesis.

Finally, to my close friends (special shout-outs to the block of cheese club and the squad) and family, I am deeply grateful for your encouragement and confidence in me. Mom and dad, you in particular have felt my joy (and pain) throughout this process. I cannot express how appreciative I am today, and every day, to have your unwavering support.

# Contents

# List of Figures

# List of Tables

# Nomenclature

## Roman Symbols

| | |
|---|---|
| $A$ | Debye-Hückel constant, $\mathrm{kg}^{\frac{1}{2}}/\mathrm{mol}^{\frac{1}{2}}$ |
| $a$ | Activity |
| $b$ | Molality, $\mathrm{mol/kg_{solvent}}$ |
| $c$ | Molarity, $\mathrm{mol/L_{solvent}}$ |
| $e$ | Faraday constant, C/mol |
| $G$ | Gibbs free energy, J |
| $\dot{G}$ | Gibbs free energy flow rate, J/s |
| $g$ | Specific Gibbs free energy, J/kg |
| $I$ | Molal ionic strength, mol/kg |
| $K_w$ | Acid dissociation constant for $H_2O$ |
| $K_2$ | Second acid dissociation constant for $H_2CO_3$ |
| $k_b$ | Boltzmann's constant, J/K |
| $M$ | Molecular weight, kg/mol |
| $m$ | Mass, kg |
| $\dot{m}$ | Mass flow rate, kg/s |
| $N_A$ | Avogadro's constant, 1/mol |
| $\dot{n}$ | Mole flow rate, kg/s |
| pH | Potential of hydrogen |
| $\dot{Q}$ | Heat rate, kg/s |
| $R$ | Correlation coefficient |
| $R^2$ | Coefficient of determination |
| $R_g$ | Universal gas constant, J/mol-K |
| $r$ | Recovery ratio, mass basis, kg/kg |
| $\bar{r}$ | Recovery ratio, mole basis, mol/mol |
| $S$ | Salinity, $\mathrm{kg_{solute}/kg_{solution}}$ |
| $\dot{S}_{gen}$ | Entropy generation flow rate, J/s-K |
| $T$ | Temperature, K |

| | |
|---|---|
| $\dot{W}$ | Work rate (power), J/s |
| $x$ | Mole fraction, kg/kg |
| $z$ | Valence of ion |

## Greek Symbols

| | |
|---|---|
| $\epsilon_o$ | Relative permittivity/dielectric constant |
| $\epsilon_r$ | Permittivity of free space, F/m |
| $\gamma$ | Activity coefficient |
| $\mu$ | Chemical potential, J/mol |
| $\nu$ | Stoichiometric coefficient |
| $\phi$ | Molal osmotic coefficient |
| $\rho_w$ | Density, kg/m$^3$ |

## Subscripts

| | |
|---|---|
| $a$, $A$, $X$ | Anion |
| $b$ | Brine |
| $CO_3$ | Carbonate |
| $c$, $C$, $M$ | Cation |
| $e$ | Environment |
| $f$ | Feed |
| H | Hydrogen |
| $HCO_3$ | Bicarbonate |
| $i$ | Species |
| *least* | Reversible operation |
| $p$ | Product |
| $s$ | Electrolyte salt species |
| *sep* | Separation |
| $w$, $H_2O$ | Water |

## Superscripts

| | |
|---|---|
| min | Minimum |
| $o$ | Standard state |

## Acronyms

| | |
|---|---|
| Alk | Alkalinity, eq/L |
| BGW | Brackish groundwater |
| SC | Specific conductance, $\mu$S/cm |
| TDS | Total dissolved solids, mg/L |

# Chapter 1

# Motivation and background

## 1.1 The water crisis in the United States

The growth of the world's population has increased the global water demand, stressing the renewable fresh water supply. In 2015, the United Nations [1] estimated that a staggering 1.8 billion people, a fourth of the global population, do not have access to water safe enough for consumption. An even more staggering 2.4 billion people, more than one-third of the world's population, lack access to basic sanitation facilities. These water deficits are only expected to worsen with time due to explosive population growth and climate change [1]. Consequently, methods to improve the quality and supply of water have become more critical for both developed and developing nations.

In tandem with the global water crisis, large parts of the United States are expected to experience high to extreme risks in sustaining the necessary water supply by 2050, as can be seen in Fig. 1-1. These high-risk areas primarily fall in high plains and southwestern states and in portions of Florida and the Mississippi Valley. Many of these drier regions are landlocked, emphasizing the potential for groundwater to play an important role in addressing national water supply needs. Surface water has remained the dominant source of the national water supply since the 1950s [2], despite a recent U.S. Geological Survey (USGS) revealing the large, untapped potential of groundwater as a water source [3]. Since most groundwater has salinity greater than 0.5 g/kg [4], it requires desalination before use for lower salinity applications, such as

drinking water and many forms of irrigation.

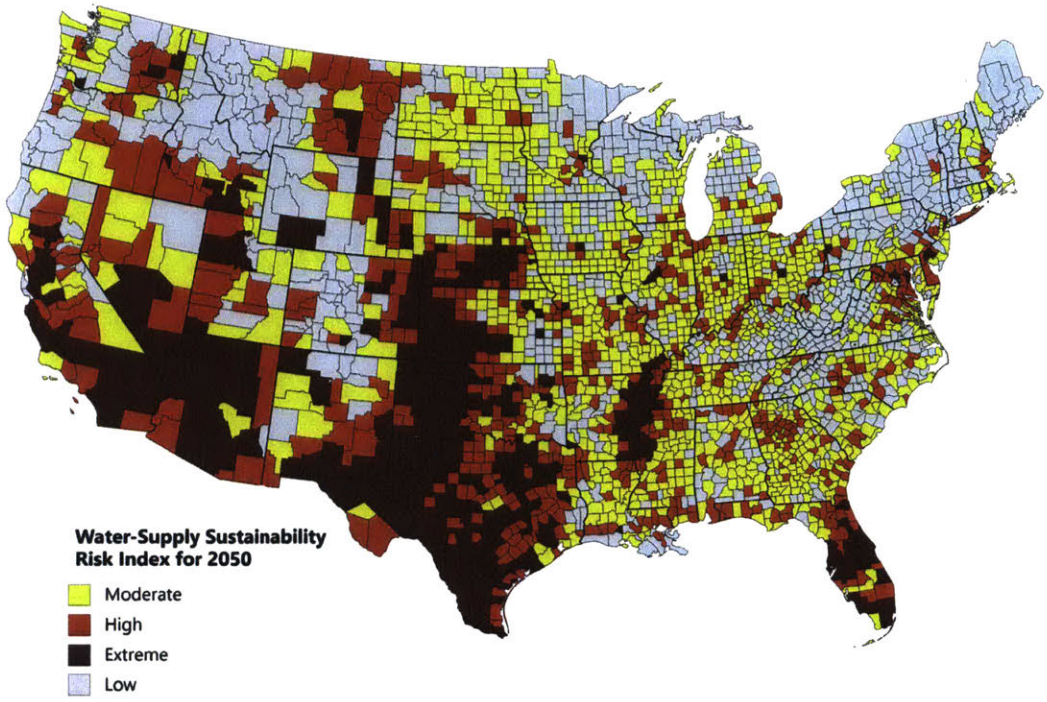


Figure 1-1: Map of water-supply-sustainability risk index for 2050 across the U.S. The index relates water demand to population growth, increases in power generation, and climate change for the year 2050 (data from [3, 5]).

## 1.2 Water use in the United States

Since 1950, the U.S. Geological Survey has conducted studies on water use in the United States every 5 years. Most recently, USGS published in 2014 a study on national water use in 2010 [2]. Historical trends and 2010 trends in water withdrawals and water demand are explored. They show the potential for growth in saline groundwater use, particularly in the brackish groundwater range. USGS defines freshwater as containing less than 1,000 mg/L of total dissolved solids (TDS), saline water as containing greater than or equal to 1,000 mg/L of TDS, and brackish water, a subset of saline water, as containing 1,000 mg/L - 10,000 mg/L of TDS [3].

### 1.2.1 Water use from 1950 to 2010

Figure 1-2 includes population and total withdrawals by water source from 1950 to 2010. Population steadily increased, while surface water remained the primary water source compared to groundwater. An upward trend in total water withdrawals occurred from 1950 to 1980, after which withdrawals remained at relatively the same magnitude until 2010. Total withdrawals in 2010 were 13% less than in 2005 [2]. Fresh surface water, fresh groundwater, and saline surface water withdrawals in 2010 decreased by 15%, 4%, and 24%, respectively, compared to in 2005 [2].

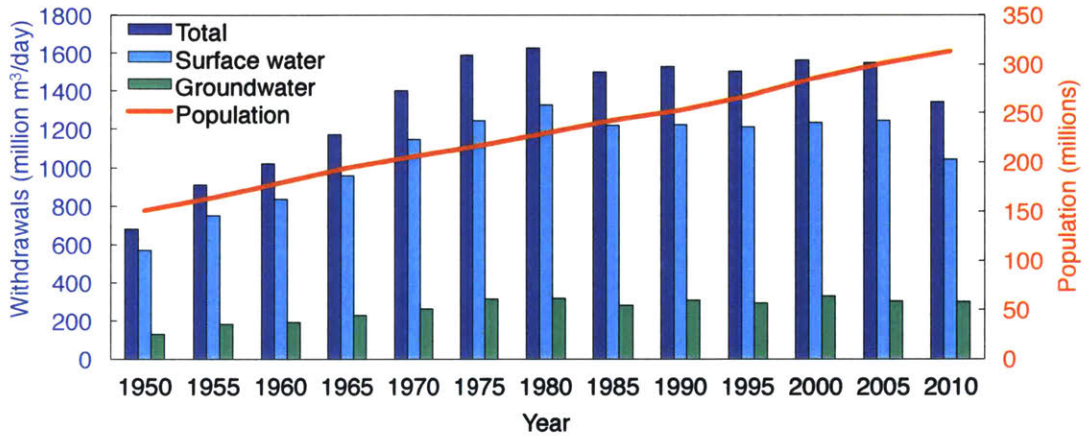


Figure 1-2: Trends in population growth and in total water, groundwater and surface water withdrawals from 1950 to 2010 in the United States (data from [2]).

The water supply in the U.S. is divided among the following categories: irrigation, thermoelectric power, public supply, domestic, livestock, industry, mining, and aquaculture [2]. Figure 1-3 shows the breakdown of total withdrawals by each of these water uses. Irrigation and thermoelectric power require the largest amount of water, while rural, domestic, and livestock require the least amount of water. Thermoelectric power and irrigation withdrawals in 2010 were 20% and 9% less than in 2005, respectively [2]. Other sectors experienced similar reductions in their water use, specifically: public supply (5%); self-supplied domestic (3%); self-supplied industrial (12%); and livestock (7%). Only the mining (39%) and aquaculture (7%) sectors reported larger withdrawals in 2010 compared to 2005 [2].

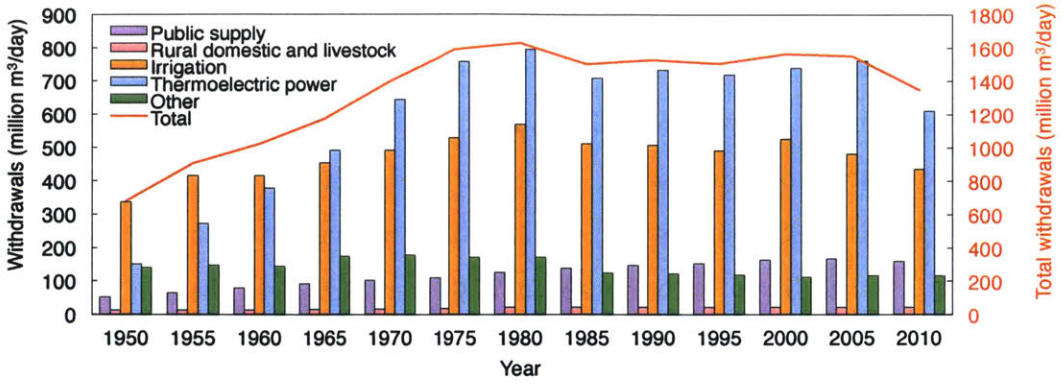


Figure 1-3: Trends in total water withdrawals and in water use from 1950 to 2010 in the United States (data from [2]).

### 1.2.2 Water use in 2010

According to the 2010 USGS study [2], total water withdrawals that year amounted to over 1,340 million $m^3$/day. Approximately 86% of total supply was derived from freshwater. Thermoelectric power, irrigation and public supply comprised 38%, 38% and 14%, respectively, of total freshwater withdrawals. The remaining 14% of total supply was saline, primarily seawater and brackish coastal water used for cooling purposes in thermoelectric power generation. In addition to withdrawals by salinity, we explore withdrawals by water source, shown in Fig. 1-4. Approximately 1,041 million $m^3$/day, or 78% of total water supply, comes from surface water, while the remaining 22%, or 300 million $m^3$/day, comes from groundwater. The majority of both surface water (84%) and groundwater (96%) is fresh. Only 4% of groundwater withdrawals contains over 1,000 mg/L of TDS. However, a 2017 USGS study [3] reveals that the volume of brackish groundwater available is over 800 times the amount of saline groundwater used each year and over 35 times the amount of fresh groundwater used. As a result, brackish groundwater is a relatively untapped source that may be capitalized on to meet the growing water demand nationwide.

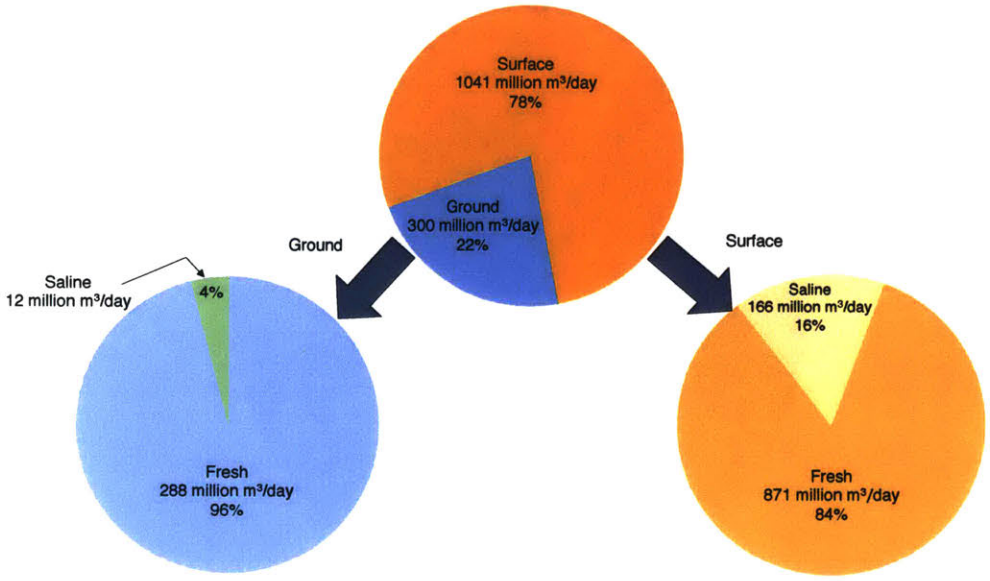


Figure 1-4: Total water withdrawals in 2010 by water source and salinity (data from [2]).

The following 12 states accounted for over 50% of total withdrawals in the country: California, Texas, Idaho, Florida, Illinois, North Carolina, Arkansas, Colorado, Michigan, New York, Alabama, and Ohio. California accounted for 11% of total withdrawals and 10% of total freshwater withdrawals for all categories nationally. Texas accounted for approximately 7% of total withdrawals for all categories, primarily for thermoelectric power, irrigation, and public supply. The largest amount of saline water withdrawals (18%) occurred in Florida, predominantly surface water withdrawals for thermoelectric power. Approximately 70% of total saline groundwater withdrawals were in Oklahoma and Texas, mostly for mining purposes.

### 1.2.3 Water quality requirements based on water use

Figure 1-5 shows that thermoelectric power, irrigation and public supply comprised 90% of total water demand in 2010. Consequently, efforts to improve the national water supply should focus on these three sectors.

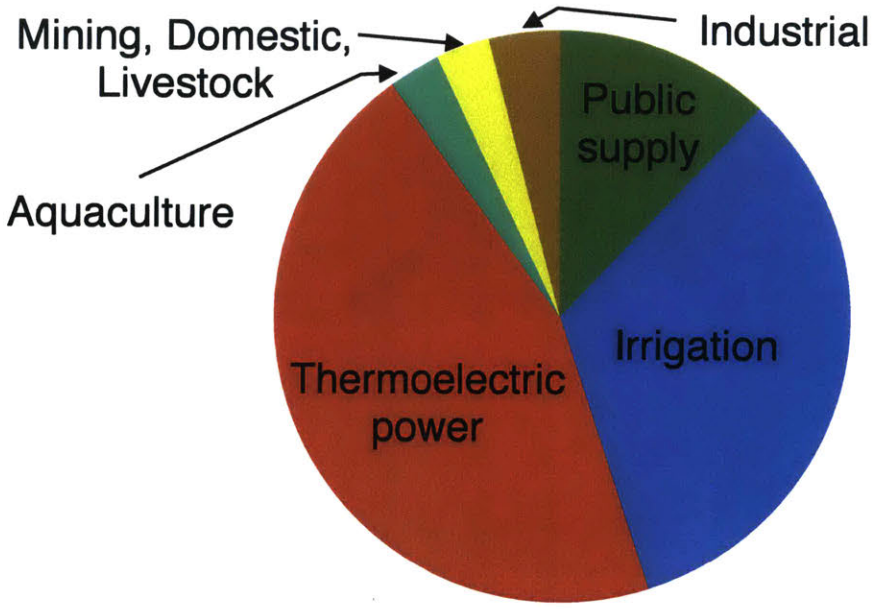


Figure 1-5: Total water withdrawals in 2010 by water use (data from [2]).

Thermoelectric power production has the highest water use in the United States and one of the highest worldwide due to its cooling requirements. It accounted for 45% of total water use in 2010 [2]. Water used to cool power-producing equipment does not have a low TDS condition. Consequently, both fresh and brackish groundwater are directly utilized in this application [2].

Irrigation of agricultural crops has the second largest water use, representing 38% of total water supply in 2010 [2]. Irrigation in California, Arkansas, Texas, and Nebraska accounted for the majority (65%) of fresh groundwater withdrawals, and required three times as much freshwater as the next largest groundwater use, public supply [2]. Water quality limitations for irrigation result from dissolved solids concentration, the relative amounts of solutes, and specific constituents, which can be damaging to crops. First, high salinity water in the plant's root zone increases the osmotic pressure of the solution in soil and decreases the plant's water absorption rate. Reduced water absorption partially or entirely prevents plant growth, compromising plant yield and seed germination [6]. TDS of less than 450 mg/L poses no potential irrigation problem [7]. TDS ranging from 450 - 2,000 mg/L slightly to mod-

erately restricts water use for irrigation, while TDS greater than 2,000 mg/L of TDS severely limits water availability for irrigation [7]. Second, water sodicity, the amount of sodium present in water, affects soil permeability, which in turn jeopardizes the irrigation process. Water with sodium concentration exceeding calcium concentration by a factor of three can lead to soil dispersion and structural breakdown. These impede the infiltration and free movement of water and air through the soil [7]. Problems associated with excessive sodium include poor seedling emergence, soil crusting, lack of aeration and plant and root diseases [8]. Finally, high concentrations of specific constituents, including boron, heavy metals, chloride or sodium, are toxic to specific crops and stunt their growth accordingly [6, 7].

Public supply (i.e., water withdrawn and delivered to homes, businesses and schools by privately operated or government-run facilities) fulfills the majority of the population's daily water needs. Drinking water falls into this category. Specific constituents in water that are toxic to humans (and livestock) include: arsenic, uranium, nitrate, boron, barium, fluoride, strontium, and manganese [3]. High dissolved solids concentration also limits water use for human consumption. The Environmental Protection Agency (EPA) recommends that drinking water contain less than 500 mg/L of total dissolved solids [9].

## 1.3 Desalination in the United States

Using brackish groundwater, a largely untapped resource, can relieve growing water pressure in water-stressed areas across the United States. For high-quality water requirements, such as in irrigation and drinking water, desalination is one technique that can be employed to treat salty groundwater before use. In 2010, 649 desalination plants were active in the United States with a combined capacity of approximately 772,000 $m^3$/day [3]. Of the total desalination capacity, 18% was for industry, 9% for power generation, 67% for municipal use and the remaining 6% for other purposes [10]. A series of surveys performed between 1971 and 2010 identified 324 municipal desalination facilities, each producing a minimum of 94 $m^3$/day [11]. More than 80%

of these plants are inland groundwater facilities, primarily located in Florida, California and Texas [11]. The majority of municipal desalination treats groundwater in the brackish salinity range [11]. Treated feedwater for municipal supply typically contains less than 3000 mg/L of TDS and rarely contains greater than 10,000 mg/L of TDS [3], largely due to increased desalination costs with increasing TDS. However, technological advancements have decreased the cost and energy requirements of desalination, and desalination has therefore become a more feasible option for applications requiring lower dissolved solids concentrations [10]. The rapid growth in the number of municipal facilities since 1971 reflects this feasibility. Brackish water municipal desalination increased from less than 10 facilities in 1971 to over 200 facilities in 2010, as can be seen in Fig. 1-6. Therefore, the infrastructure necessary for small and large-scale brackish groundwater desalination is already well-established in the U.S.

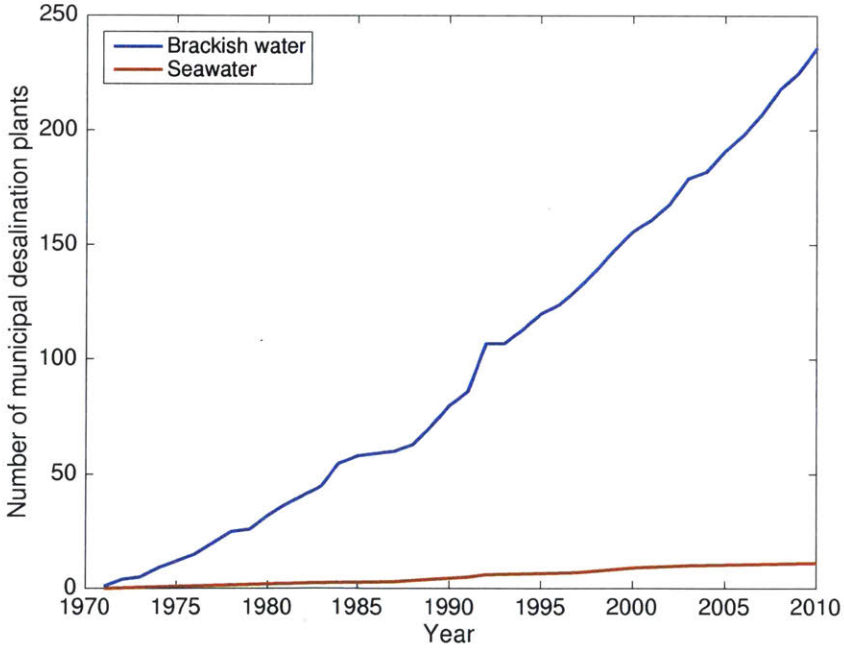


Figure 1-6: Number of municipal desalination reverse osmosis plants by feedwater type (data in [11]). Reverse osmosis is the most widely used form of desalination in the U.S. [3].

## 1.4 Minimum energy requirements for brackish groundwater desalination to meet low salinity water demand in the United States

Exploiting brackish groundwater (BGW), a widely available but minimally used resource, can play a key role in addressing risks to sustaining the necessary water supply in the United States, particularly in inland areas. It can be directly used in applications that do not require a high-quality supply, or it can be indirectly used after desalination to provide an alternative water source in regions with limited or unavailable freshwater. Despite BGW potential to relieve mounting pressure on freshwater supplies, brackish groundwater has been studied far less than seawater as a water source. A 1965 study conducted by U.S. Geological Survey served as the primary source of information on the national distribution of brackish groundwater until USGS published an updated national assessment on the resource's distribution in 2017 [3]. Moreover, comprehensive assessments on BGW desalination energy costs are absent in the literature. Since ionic groundwater composition varies greatly from location to location, unlike seawater [12] (refer to Table 1.1), conducting a large-scale analysis of the resource's energy costs is crucial.

| Constituent | Normal Seawater | Brackish Groundwater |
|---|---|---|
| Bicarbonate | 140 | 385 |
| Boric Acid | 26 | - |
| Bromide | 65 | - |
| Calcium | 400 | 258 |
| Chloride | 18,980 | 870 |
| Fluoride | 1 | - |
| Iodide | <1 | - |
| Iron | - | <1 |
| Magnesium | 1,262 | 90 |
| Manganese | - | 1 |
| Nitrate | - | 1 |
| Phosphate | - | <1 |
| Potassium | 380 | 9 |
| Silica | - | 25 |
| Silicate | 1 | 25 |
| Sodium | 10,556 | 739 |
| Strontium | 13 | 3 |
| Sulfate | 2,649 | 1,011 |
| Other | 1 | - |
| Total Dissolved Solids | 34,483 | 3,394 |

Table 1.1: Characteristic seawater and brackish water compositions (data in [13]). Highlighted rows indicate primary constituents.

This thesis performs a national investigation of BGW characteristics and minimum desalination energy costs in the continental United States, using the U.S. Geological Survey's 2017 major-ions groundwater dataset [14]. In this thesis, we define brackish groundwater as containing 500 - 10,000 mg/L of total dissolved solids. First, the site-specific least work of separation is calculated and mapped for approximately 28,000 BGW samples across the country. The least work of separation represents a baseline for specific energy consumption (SEC) of real-world desalination systems. Figure 1-7 shows that SEC is usually 2-5 times greater than the least work of separation, depending on system design aspects such as plant size and configuration. Areas with high water stress and low least work requirements are mapped to highlight regions with desalination potential. The least work of separation calculations are then used to develop simplified equations between least work and TDS, specific conductance, ionic strength and molality. Lastly, the thesis explores the impact of groundwater composition on the least work of separation, and the geographic distribution of TDS and well depth for 46,000 BGW samples and major ions for 28,000 BGW samples.

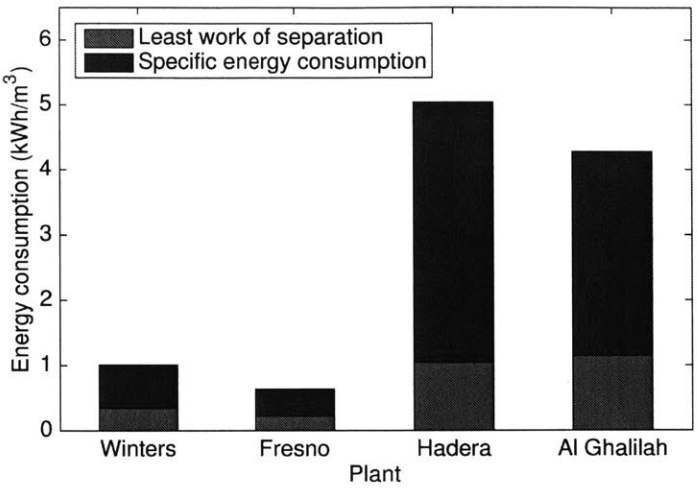


Figure 1-7: Least work of separation as a percentage of specific energy consumption for two brackish water reverse osmosis plants (BWRO), Winters and Fresno, and two seawater reverse osmosis plants (SWRO), Hadera and Al Ghalilah. The darker regions represent the additional energy generated by irreversibilites in RO systems, primarily resulting from the driving pressure drop across the membranes. Data on SEC, recovery ratio and feed and product salinities was obtained from DesalData [15]. Seawater composition was acquired from WHO [13]. Characteristic brackish groundwater composition was acquired from USGS based on BWRO plant location [14].

# Chapter 2

# U.S. Geological Survey major-ions dataset

The U.S. Geological Survey (USGS) compiled a dataset of the major ions in groundwater in 2017 [14] to provide an updated summary of the occurrence of BGW and a more complete characterization of BGW resources. The dataset contains chemical, physical, and geographic properties of groundwater from 16 sources for approximately 124,000 groundwater samples across the continental U.S., Alaska, Hawaii, Puerto Rico, the U.S. Virgin Islands, Guam, and American Samoa. This paper uses brackish groundwater data from the continental U.S. only.

## 2.1 Coverage

The geochemical sources used to compile the major-ions dataset range from single publications to large datasets and from state studies to national assessments. Specific information on these sources can be found in Appendix A. Groundwater properties in the dataset include the concentrations of dissolved solids, major ions, trace elements and radionuclides, pH, temperature, specific conductance, and density. Many of these properties are necessary to evaluate the least work of separation. Some samples have missing density or bicarbonate and/or carbonate concentration data. In these cases, density was calculated using a well-established correlation for density,

temperature and salinity [16]. Alkalinity was converted to bicarbonate and carbonate concentrations according to methods outlined by Stumm and Morgan [17], using the Debye-Hückel limiting law [18]. The dataset also contains a latitude and longitude pair for each sample, enabling geographic distribution analyses of groundwater characteristics.

Approximately 78,000 samples are freshwater (TDS < 500 mg/L) and 46,000 samples are brackish water. Of the brackish samples, 28,000 have complete composition data, not diverging from electroneutrality by more than 5% [1]. Groundwater samples are drawn from all 50 states. New Jersey, Delaware, Maryland, Texas, and North Dakota have the highest well/area densities (wells/km$^2$) in the dataset, while Kentucky, Oregon, New Mexico, Alabama, and Vermont have the lowest in the dataset. North Dakota, South Dakota, Montana, Wyoming, and Nebraska have the highest well/population densities (wells/person) in the dataset, while Kentucky, Alabama, Georgia, Vermont, and Rhode Island have the lowest in the dataset.

## 2.2 Limitations

Although the dataset covers large areas across the country, it has some limitations. USGS was unable to compile all available groundwater data for the nation, particularly from local sources. The agency relied primarily on larger datasets available in a digital format from state organizations. In addition, well selection biases influence the type of groundwater data that is available. Well sites are not methodologically selected to characterize whole aquifers. Rather, they tend to be drilled in areas that have freshwater and/or a lower depth requirement to tap into the resource. This preference for freshwater and shallow wells results in a lack of comprehensive and consistent data. Consequently, the dataset does not represent a complete characterization of BGW resources in the U.S.

The majority of samples have a TDS less than 500 mg/L, and there is an uneven

[1]The percent deviation from electroneutrality is calculated by summing over all of the cation $C$ and anion species $A$ in the distributed solution, using the charge $z$ of each species: pct err = $100\frac{\sum_C (z \cdot C) - \sum_A (z \cdot |A|)}{\sum_C (z \cdot C) + \sum_A (z \cdot |A|)}$ [14].

distribution of wells across the 50 states, resulting in data gaps for many parts of the nation. The low correlation coefficient of 0.31 between state area and number of wells per state reflects that the occurrence of wells in a given area varies across states. This non-uniform well distribution may result partly from population density and total groundwater withdrawals in a given area. The correlation coefficients of number of wells per state, with state population and with total state groundwater withdrawals, are 0.53 and 0.60, respectively; these values indicate that number of wells in a state is related to these two parameters. Figure 2-1 shows the total groundwater withdrawals per state in 2010 versus the number of groundwater samples per state in the major-ions dataset. Texas and California have both the highest number of samples and total groundwater withdrawals, while Rhode Island and Vermont have the smallest number of samples and total groundwater withdrawals.

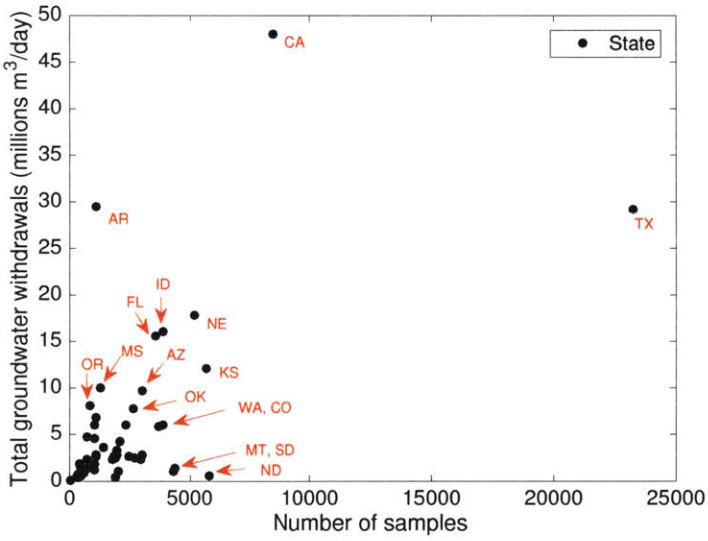


Figure 2-1: Total annual groundwater withdrawals per state in 2010 (data in [2]) versus number of samples per state in USGS major-ions dataset. Each dot corresponds to a state. Red labels are used to specify 16 of the 48 states in the contiguous U.S.

In order to fully characterize BGW resources, a larger amount of existing groundwater data must be compiled. New data that has a more extensive geographic reach and less bias towards shallow and freshwater samples must be collected. Increased hydraulic analyses must be conducted.

# Chapter 3

# Methodology

The least work of separation is the benchmark energy consumption for any desalination system. It represents the minimum amount of work required to separate the supplied water into pure and brine streams leaving the desalination process, as determined for a thermodynamically ideal (reversible) process. The USGS data in combination with the mixed electrolyte Pitzer model [19, 20] is used to compute the difference in chemical potential [21] of these streams, which determines the least work of separation for each groundwater sample. In this thesis, the least work is calculated per unit of product produced ($\dot{m}_p = 1$ kg/s) and written as $\dot{W}_{least}/\dot{m}_p$ (kWh/m$^3$).

## 3.1 Derivation of least work of separation

The least work of separation on a mass basis is derived from a control volume surrounding a black-box separator. The desalination system is modeled as a black-box separator with an inlet stream, the feed ($f$), and two outlet streams, the brine ($b$) and the product ($p$), as shown in Fig. 3-1. All streams have different salinities $S$. A control volume is chosen far enough away from the separator that the inlet and outlet streams are at ambient pressure and temperature, $T_e$. The heat entering the system at environmental temperature is $\dot{Q}$, and the rate of work done on the system to cause separation is $\dot{W}_{sep}$. Mistry et al. [22] provide a detailed discussion regarding this choice of control volume.

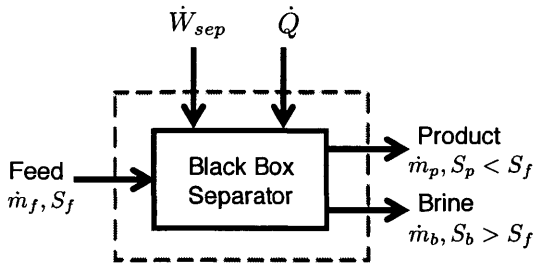


Figure 3-1: A control volume of a desalination system modeled as a black-box separator for deriving least work of separation.

Combining the first and second laws of thermodynamics on this control volume gives the rate of work for separation:

$$\dot{W}_{sep} = \dot{m}_p g_p + \dot{m}_b g_b - \dot{m}_f g_f + T_e \dot{S}_{gen} \tag{3.1}$$

where $g_j$ is the specific Gibbs free energy per kilogram of solution, $\dot{m}_j$ is the mass flow rate of stream $j$ and $\dot{S}_{gen}$ is the total entropy generated by the separation process within the control volume. The least work of separation represents the minimum amount of work required for separation, which occurs when the entropy generation is zero, i.e., for reversible operation [21]:

$$\dot{W}_{least} = \dot{m}_p g_p + \dot{m}_b g_b - \dot{m}_f g_f \tag{3.2}$$

Therefore, the difference between least work of separation and actual specific energy consumption results from irreversibilities generated in real-world desalination systems. Entropy generation for thermal desalination systems primarily sources from heat transfer across a finite temperature difference, while entropy generation for membrane desalination systems mainly results from water transport through the high pressure drop across the membrane [22]. For a given salinity, water composition effects do not substantially impact entropy generation [22]. Conservation of mass for the mixture and the salts yields the least work of separation per mass flow rate of

product stream in terms of mass recovery ratio:

$$\frac{\dot{W}_{least}}{\dot{m}_p} = (g_p - g_b) - \frac{1}{r}(g_f - g_b) \tag{3.3}$$

where the mass recovery ratio is defined as the ratio of the mass flow rate of product stream to the mass flow rate of feed stream:

$$r = \frac{\dot{m}_p}{\dot{m}_f} \tag{3.4}$$

We can gain more insight into the effect of physical properties on the least work of separation by rewriting Eq. (3.1) on a molar basis [21, 22]:

$$\begin{aligned}\frac{\dot{W}_{least}}{\dot{n}_{H_2O,p}RT} = &\left(\ln\frac{a_{H_2O,p}}{a_{H_2O,b}} + \sum_s b_{s,p}M_{H_2O}\ln\frac{a_{s,p}}{a_{s,b}}\right) \\ &-\frac{1}{\bar{r}}\left(\ln\frac{a_{H_2O,f}}{a_{H_2O,b}} + \sum_s b_{s,f}M_{H_2O}\ln\frac{a_{s,f}}{a_{s,b}}\right)\end{aligned} \tag{3.5}$$

where M is molar mass, $b$ is molality in mol/kg, subscript $s$ represents all binary salt species in the mixture, $a$ represents the activities of solutes and solvent in each stream, and the molar recovery ratio $\bar{r}$ is defined as the ratio of molar flow rate of water in product stream to molar flow rate of water in feed stream:

$$\bar{r} = \frac{\dot{n}_{H_2O,p}}{\dot{n}_{H_2O,f}} \tag{3.6}$$

Least work of separation is a function of feed and product composition, recovery ratio, and ambient pressure and temperature [21, 22]. In this thesis, least work results are provided for a pure product ($a_{H_2O,p} = 1$, $b_{s,p} = 1$ in Eq. (3.5)) at atmospheric pressure and evaluated at zero recovery. The USGS dataset includes the temperatures of each water sample, used in least work calculations. As recovery ratio approaches zero (i.e., infinitesimal extraction), least work of separation is minimized [21]:

$$\dot{W}_{least}^{min} = \lim_{r\to 0}\dot{W}_{least}$$

This is known as the minimum least work, and is the efficiency datum for drinking water desalination systems. This thermodynamic limit is equivalent to the removal of a drop of pure water from the ocean, which acts as a reservoir of chemical potential (analogous to a thermal reservoir in heat engine theory). Seawater from this reservoir is used as feedwater to the desalination system, and brine leaving the system is disposed into the same reservoir. Consequently, the feed and brine streams share the same chemical properties, resulting in identical Gibbs free energies [21]. The second term in Eqs. (3.3) and (3.5) becomes zero divided by zero. The mathematical proof in Appendix B shows that these terms limit to zero, so that Eqs. (3.3) and (3.5) reduce to the difference in Gibbs free energy of the product and brine streams:

$$\frac{\dot{W}_{least}^{min}}{\dot{m}_p} = (g_p - g_b) \tag{3.7}$$

For a sufficiently large BGW aquifer, brine disposal will not affect aquifer salinity, implying the aquifer acts as a reservoir of chemical potential in the same manner as the ocean. In such cases, the above physical argument holds for BGW desalination systems as well. However, the theoretical definition of minimum least work is general and does not require the actual presence of a disposal system for its validity. Thus, it remains a robust metric for describing the energy requirements to desalinate groundwater from any well.

## 3.2 Calculations

### 3.2.1 Evaluation of activity coefficients for least work of separation using Pitzer mixed electrolyte model

The Pitzer mixed electrolyte model [19, 23, 24] is used to calculate activities of solvent and solutes in each groundwater sample to determine the least work of separation.

The Gibbs free energy of a mixture is written as:

$$G = \sum_i n_i \mu_i \tag{3.8}$$

where $n_j$ is the number of moles and $\mu_i$ is the chemical potential of species $i$. Chemical potential is:

$$\mu_i = \mu_i^\circ + R_g T \ln(a_i) \tag{3.9}$$

where $\mu_i^\circ$ is the chemical potential in the standard state, $R_g$ is the universal gas constant, $T$ is the temperature, and $a_i$ is the activity of species $i$. The solute activity is defined on a molal scale as:

$$a_i = \gamma_i b_i \tag{3.10}$$

where $b_i$ is the molality of ion species $i$ and $\gamma_{b,i}$ is the activity coefficient. The activity coefficient of an individual cation, $M$, is written as:

$$\begin{aligned} \ln \gamma_M = {} & z_M^2 F + \sum_a b_a (2B_{Ma} + ZC_{Ma}) \\ & + \sum_c b_c (2\Phi_{Mc} + \sum_a b_a \Psi_{Mca}) \\ & + \sum_{a<a'} \sum b_a b_{a'} \Psi_{aa'M} \\ & + |z_M| \sum_c \sum_a b_c b_a C_{ca} + \sum_n b_n (2\lambda_{nM}) \end{aligned} \tag{3.11}$$

For an individual anion, $X$, the equation is analogous to Eq. (3.11):

$$\begin{aligned} \ln \gamma_X = {} & z_X^2 F + \sum_c b_c (2B_{cX} + ZC_{cX}) \\ & + \sum_a b_a (2\Phi_{Xa} + \sum_c b_c \Psi_{Xac}) \\ & + \sum_{c<c'} \sum b_c b_{c'} \Psi_{cc'X} \\ & + |z_X| \sum_c \sum_a b_c b_a C_{ca} + \sum_n b_n (2\lambda_{nX}) \end{aligned} \tag{3.12}$$

The activity coefficient of an uncharged species $N$ (e.g., aqueous $CO_2$) is given by:

$$\ln \gamma_N = \sum_c b_c(2\lambda_{Nc}) + \sum_a b_a(2\lambda_{Na}) \tag{3.13}$$

The activity of water on a molal scale can be expressed as:

$$\ln(a_{H_2O}) = -\frac{M_w(\sum_i b_i)\phi}{1000} \tag{3.14}$$

Molal osmotic coefficient $\phi_b$ is computed from the expression:

$$\begin{aligned}(\phi - 1)\sum_i m_i = 2\Bigg[&\frac{-A^\phi I^{3/2}}{1 + 1.2\sqrt{I}} \\ &+ \sum_c \sum_a b_c b_a (B^\phi_{ca} + ZC_{ca}) \\ &+ \sum_{c<c'} \sum b_c b_{c'} \left(\Phi^\phi_{cc'} + \sum_a b_a \Psi_{cc'a}\right) \\ &+ \sum_{a<a'} \sum b_a b_{a'} \left(\Phi^\phi_{aa'} + \sum_c b_c \Psi_{aa'c}\right) \\ &+ \sum_n \sum_a b_n b_a \lambda_{na} + \sum_n \sum_c b_n b_c \lambda_{nc}\Bigg]\end{aligned} \tag{3.15}$$

where $z$ is the species charge, $Z = \sum_i |z_i| m_i$ and $M_w$ is the molar mass of water. The remainder are functions that quantify particular solute interactions, as discussed below. Subscript $c$ represents cations other than $M$, $a$ represents anions other than $X$, and $n$ represents uncharged (neutral) solutes. Summation over all $i$, $c$, $a$, and $n$ denotes a sum over all solutes, cations, anions, and neutral solutes, respectively. The summation notations $c < c'$ and $a < a'$ indicate that the sum should be carried out over all discernible cation pairs and anion pairs, respectively.

The following equations define the terms in the Pitzer equations for the activity and osmotic coefficients in aqueous solutions. The term $F$ is based on an extended

Debye-Hückel function [18]:

$$F = -A^{\phi}\left(\frac{\sqrt{I}}{1+1.2\sqrt{I}} + \frac{2}{1.2}\ln(1+1.2\sqrt{I})\right) + \sum_{c}\sum_{a} b_c b_a B'_{ca} + \sum_{c<c'}\sum b_c b_{c'}\Phi'_{cc'} + \sum_{a<a'}\sum b_a b_{a'}\Phi'_{aa'} \tag{3.16}$$

It shows the characteristic first-order-square-root dependence on ionic strength resulting from long-range electrostatic interactions. The parameter $A^{\phi}$, which corresponds to the Debye-Hückel limiting law, is written as:

$$A^{\phi} = \frac{1}{3}\left[\frac{e^3\left(2\pi N_A \rho_{H_2O}\right)}{\left(1000\epsilon k_b T\right)^{1/2}}\right] \tag{3.17}$$

where $\rho_{H_2O}$ is the density of pure water, $N_A$ is Avogadro's number, $k_B$ is Boltzmann's constant, and $\epsilon$ is the relative permittivity of the solvent, which can be obtained from Uematsu and Franck [25]. The functions $B_{ij}$, $B'_{ij}$, $B^{\phi}_{ij}$, and $C_{ij}$ represent the interactions between cations and anions:

$$B_{MX} = \beta^{(0)}_{MX} + \beta^{(1)}_{MX} g(\alpha_{MX}\sqrt{I}) + \beta^{(2)}_{MX} g(12\sqrt{I}) \tag{3.18a}$$

$$B'_{MX} = \beta^{(1)}_{MX} g'(\alpha_{MX}\sqrt{I})/I + \beta^{(2)}_{MX} g'(12\sqrt{I})/I \tag{3.18b}$$

$$B^{\phi}_{MX} = \beta^{(0)}_{MX} + \beta^{(1)}_{MX}\exp\left(-\alpha_{MX}\sqrt{I}\right) + \beta^{(2)}_{MX}\exp\left(-12\sqrt{I}\right) \tag{3.18c}$$

$$C_{MX} = \frac{C^{\phi}_{MX}}{2|z_M z_X|^{1/2}} \tag{3.18d}$$

where $\alpha_{MX} = 2.0$ for 1-1 electrolytes and $\alpha_{MX} = 1.4$ for 2-2 and higher electrolytes. The parameters $\beta^{(i)}_{MX}$ are tabulated for a given ion pair. The parameter $\beta^{(2)}_{MX}$ is related to complex formation and typically only has a non-zero value for 2-2 electrolytes. The

functions $g(x)$ and $g'(x)$ are given by:

$$g(x) = 2(1-(1+x)e^{-x})/x^2 \tag{3.19a}$$

$$g'(x) = -\frac{2}{x^2}\left[1-\left(1+x+\frac{x^2}{2}\right)e^{-x}\right] \tag{3.19b}$$

The functions $\Phi_{ij}$ and $\Phi'_{ij}$ represent interactions between like-charged pairs:

$$\Phi_{ij} = \theta_{ij} + {}^{E}\theta_{ij}(I) \tag{3.20a}$$

$$\Phi'_{ij} = {}^{E}\theta'_{ij}(I) \tag{3.20b}$$

$$\Phi^{\phi}_{ij} = \theta_{ij} + {}^{E}\theta_{ij}(I) + I{}^{E}\theta'_{ij}(I) \tag{3.20c}$$

where $\theta_{ij}$ is the only adjustable variable for a given ion pair. The terms ${}^{E}\theta_{ij}(I)$ and ${}^{E}\theta'_{ij}(I)$ reflect excess free energy sourcing from electrostatic interactions between asymmetric electrolytes (i.e. ions with charge of same sign and different magnitude). They are dependent only on ionic strength and can be expressed as:

$${}^{E}\theta_{ij}(I) = \frac{z_i z_j}{4I}\left(J_0(x_{ij}) - \frac{1}{2}J_0(x_{ii}) - \frac{1}{2}J_0(x_{jj})\right) \tag{3.21a}$$

$${}^{E}\theta'_{ij}(I) = \frac{z_i z_j}{8I^2}\left(J_1(x_{ij}) - \frac{1}{2}J_1(x_{ii}) - \frac{1}{2}J_1(x_{jj})\right) - \frac{{}^{E}\theta_{ij}}{I} \tag{3.21b}$$

where $J_0(x)$ and $J_1(x)$ are defined as:

$$J_0(x) = \frac{1}{4}x - 1 + \frac{1}{x}\int_0^{\infty}\left[1-\exp\left(-\frac{x}{y}e^{-y}\right)\right]y^2\,dy \tag{3.21c}$$

$$J_1(x) = \frac{1}{4}x - \frac{1}{x}\int_0^{\infty}\left[1-\left(1+\frac{x}{y}e^{-y}\right)\times\exp\left(-\frac{x}{y}e^{-y}\right)\right]y^2\,dy \tag{3.21d}$$

and $x_{ij}$ is defined as:

$$x_{ij} = 6z_i z_j A^{\phi}\sqrt{I} \tag{3.21e}$$

The integrals in Eqs. (3.21c) and (3.21d) can be evaluated numerically. In conclusion, the following parameters are adjustable: 3 to 4 per unlike-charged pair, $\beta^{(0)}_{MX}$, $\beta^{(1)}_{MX}$, $\beta^{(2)}_{MX}$, and $C^{\phi}_{MX}$; one per like-charged pair, $\theta_{ij}$; and one per cation-cation-anion and

anion-anion-cation triplet, $\Psi_{ijk}$. Tabulated data on these parameters can be found in numerous sources in the literature, some of which include slightly different values [17, 19, 23, 26, 27, 28, 29]. In theory, the adjustable binary and ternary parameters ($\beta^{(i)}_{MX}$, $C^{\phi}_{MX}$, $\theta_{ij}$, and $\Psi_{ijk}$) are functions of temperature. However, complete data on these parameters as a function of temperature over the range of interest are typically unavailable in open literature (although some notable collections are accessible [19, 28, 29]). However, Silvester and Pitzer [30] have shown that the temperature derivatives of these parameters are often small. They have also noted that much of the temperature variation in activity coefficient is restricted to $A^{\phi}$ (Eq. 3.17), due to both the parameter's explicit dependence on temperature and its implicit dependence through variations in the dielectric constant [30].

### 3.2.2 Density, alkalinity, and correlation coefficient

The missing density of water samples was calculated using a one-atmosphere equation of state of seawater [16]:

$$\rho = \rho_{\circ} + AS + BS^{3/2} + CS^2 \tag{3.22}$$

where $\rho$, $A$, $B$, and $C$ are defined as:

$$\rho_{\circ} = 999.842594 + (6.793952\times10^{-2})T^2 + (1.001685\times10^{-4})T^3 - (1.120083\times10^{-6})T^4 + (6.536336\times10^{-9})T^5$$

$$A = 8.24493\times10^{-1} - (4.0899\times10^{-3})T + (7.6438\times10^{-5})T^2 - (8.2467\times10^{-7}T^3) + (5.3875\times10^{-9})T^4$$

$$B = -5.72466\times10^{-3} + (1.0227\times10^{-4})T - (1.6546\times10^{-6})T^2$$

$$C = 4.3814\times10^{-4}$$

The equation can be used for water temperature from 0 °C to 40 °C and salinity from 0.5 g/kg to 43 g/kg. Brackish groundwater temperatures and salinities fall into these ranges. Since the brackish solutions are quite dilute, all samples have a density within 0.3% of $\rho = 1$ kg/L. Alkalinity was converted to carbonate $[CO_3]^{2-}$ concentrations

for samples missing this value [17]:

$$c_{CO_3} = \frac{\text{Alk} - K_w \times 10^{\text{pH}} + \frac{10^{-\text{pH}}}{\gamma_H}}{2 + \frac{10^{-\text{pH}}}{K_2}} \tag{3.23}$$

and bicarbonate $[HCO_3]^-$ concentrations for samples missing this field:

$$c_{HCO_3} = \frac{\text{Alk} - K_w \times 10^{\text{pH}} + \frac{10^{-\text{pH}}}{\gamma_H}}{1 + 2K_2 \times 10^{\text{pH}}} \tag{3.24}$$

where Alk is alkalinity in eq/L, $c_{CO_3}$ and $c_{HCO_3}$ are concentrations in mol/L, and $K_2$ and $K_w$ are equilibrium constants depending on temperature. Analytic expressions for these constants can be found in Stumm and Morgan [17]. Activity coefficient $\gamma_H$ is calculated using the Debye-Hückel limiting law [18].

The correlation coefficient, $R$, represents the linearity of the relationship between the least work of separation $x$ and other physical and chemical properties of groundwater $y$:

$$R = \frac{\sum (x - \bar{x})(y - \bar{y})}{\sqrt{\sum (x - \bar{x})^2 \sum (y - \bar{y})^2}} \tag{3.25}$$

where $\bar{x}$ and $\bar{y}$ are the averages of the respective parameters. The coefficient is a number between -1 and 1, with unity representing a perfect linear dependence between two variables. The square of the correlation coefficient determines the coefficient of determination $R^2$, which represents how well the linear fit matches observed outcomes.

# Chapter 4

# Least work of separation

## 4.1 Geographic distribution

Least work of separation varies considerably across the U.S. Figure 4-1 illustrates the geographic distribution of the minimum least work of separation across the United States for BGW samples. We choose to map least work at 0% recovery, the minimum least work, since it is a well-established thermodynamic limit and the appropriate efficiency datum [21]. However, real-world brackish groundwater desalination systems typically operate at 75% - 90% recoveries [31].[1] Least work of separation at these higher recoveries is greater than minimum least work by a factor of 1.6-2.7 for brackish groundwater samples in the dataset. This factor increases for higher salinity water (TDS > 10,000 mg/L). Figure 4-2 shows how least work of separation increases with recovery ratio and total dissolved solids. A characteristic seawater solution curve is included for comparison to brackish groundwater. A 35,000 mg/L mixture has a minimum least work of separation of approximately 0.74 kWh/m$^3$, over 3 times the amount of a 10,000 mg/L brackish solution. Table 4.1 includes least work of separation evaluated at 0%, 50%, 70%, and 90% recovery for various brackish and seawater solutions, including those in Fig. 4-2.

[1] An important consideration in operating BGW membrane-based desalination systems at higher recoveries is scale formation on membranes. A commonly used metric to measure scaling potential of a groundwater sample is the saturation index. Information on the saturation indexes of 28,000 BGW samples for which least work of separation is computed can be found in Appendix D.

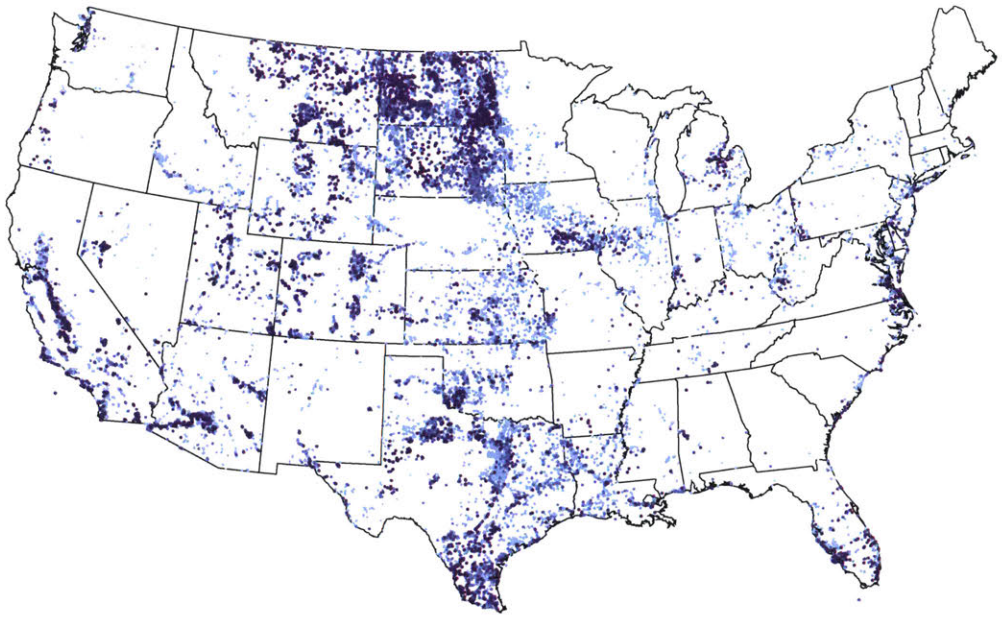

(a)

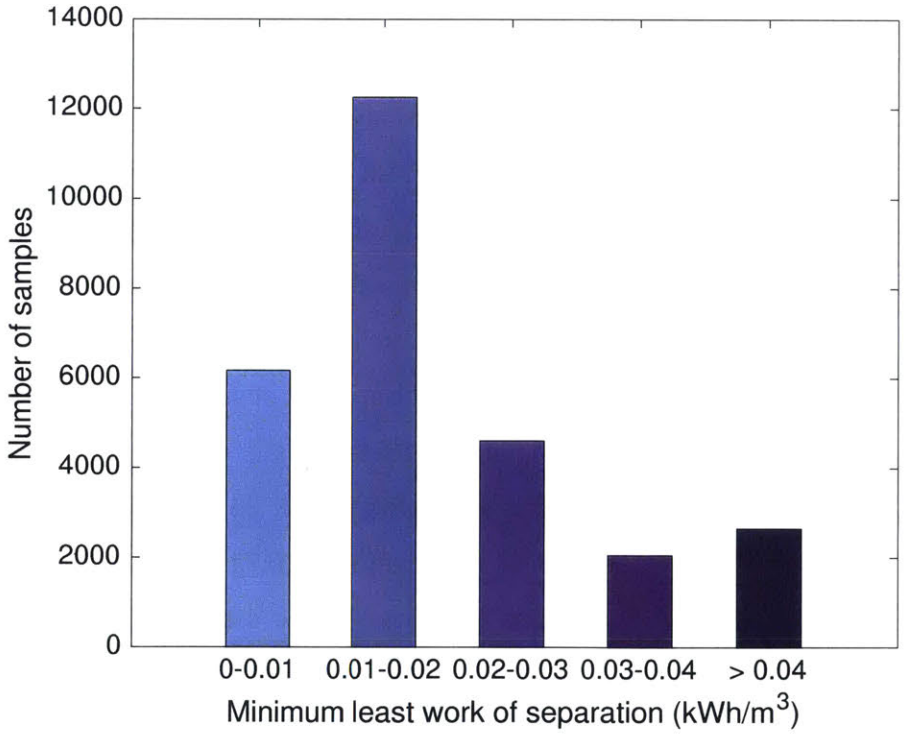


(b)

Figure 4-1: Map of minimum least work of separation (evaluated at 0% recovery) for 28,000 BGW samples with complete composition data. Each dot represents a groundwater sample. White areas indicate a lack of ion composition data. Additional least work of separation maps can be found in Appendix E.

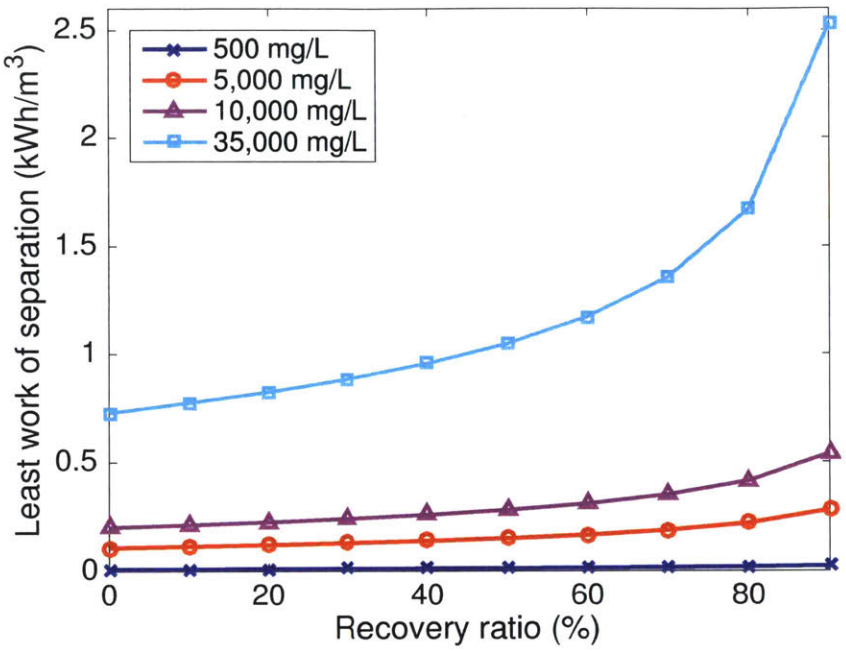


Figure 4-2: Least work of separation as a function of recovery ratio ranging from 0%-90% and TDS for one seawater solution and three brackish groundwater solutions with different compositions. The 500 mg/L solution contains the following major ions: Cl = 110 mg/L; Na = 110 mg/L; $SO_4$ = 110 mg/L; and $HCO_3$ = 110 mg/L. The 5,000 mg/L solution contains the following major ions: Cl = 2,950 mg/L; Na = 1,840 mg/L; and $HCO_3$ = 362 mg/L. The 10,000 mg/L solution contains the following major ions: Cl = 5,400 mg/L; Na = 3,000 mg/L; and $SO_4$ = 800 mg/L.

Table 4.1: Least work of separation in kWh/m$^3$ at 0%, 50%, 70%, and 90% recovery $r$ for brackish and seawater solutions containing different total dissolved solids concentrations.

| TDS | $r$ = 0% | $r$ = 50% | $r$ = 70% | $r$ = 90% |
|---|---|---|---|---|
| 500 mg/L | 0.0084 | 0.012 | 0.014 | 0.021 |
| 2,500 mg/L | 0.050 | 0.069 | 0.086 | 0.13 |
| 5,000 mg/L | 0.11 | 0.15 | 0.19 | 0.28 |
| 7,500 mg/L | 0.15 | 0.20 | 0.25 | 0.38 |
| 10,000 mg/L | 0.20 | 0.28 | 0.35 | 0.54 |
| 35,000 mg/L | 0.74 | 1.0 | 1.4 | 2.5 |

Figure 4-3 shows the water stress level of the BGW samples for which least work of separation is calculated. Water stress measures the ratio of total withdrawals to total available renewable supply in a given area annually [32]. Many samples are located in areas experiencing high or extremely high levels of water stress, i.e., a large disparity between water supply and water demand.

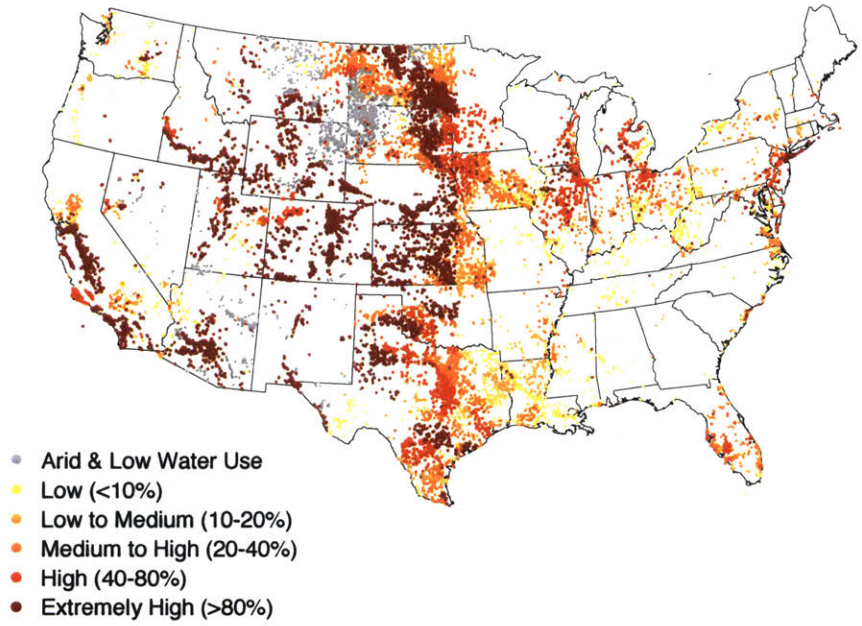


Figure 4-3: Map of water stress levels across the continental United States for 28,000 BGW samples (data in [32]). Water stress is defined as: water stress = $100\ \frac{\text{total annual water withdrawals}}{\text{total annual renewable supply}}$. A higher percentage indicates that more water users are competing for a limited water supply. For example, in extremely high stress areas, more than 80% of water available to domestic, agricultural and industrial users is withdrawn annually.

Groundwater samples that fall in the two highest water stress brackets from Fig. 4-3 and the two lowest least work of separation brackets from Fig. 4-1 are mapped in Fig. 4-4. Least work of separation represents a baseline of energy costs required for desalination, independent of technology used, while high water stress indicates

that more water users are competing for a limited water supply. Therefore, Fig. 4-4 highlights regions that hold higher potential for desalination to play a role in reducing the gap between high water demand and low water supply. [2]

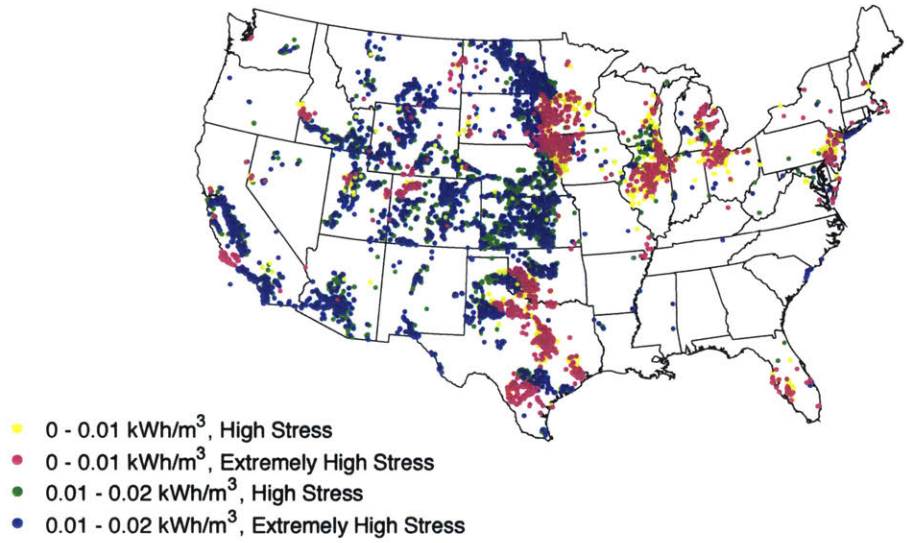


Figure 4-4: Map of BGW samples that fall into two lowest least work of separation brackets from Fig. 4-1 and the two highest water stress brackets from Fig. 4-3. Each dot represents a BGW sample, and each color represents a pair of least work and water stress brackets. Clusters of dots suggest areas that hold high potential for desalination. Additional desalination potential maps can be found in Appendix E.

[2]These areas can be found in the following states and/or principal aquifers: Basin and Range basin-fill aquifers in south-central California and southern Arizona; Central Valley aquifer and California Coastal Basin aquifers in central and southern California; Colorado Plateaus aquifer in north-central Colorado; along the border of the Dakotas and Nebraska with Minnesota and Iowa; High Plains aquifer spanning the Texas Panhandle, Kansas and Nebraska; Coastal Plain aquifer systems in South Texas; Blaine, Rush springs and Central Oklahoma aquifers in west and central Oklahoma; Snake River Plain aquifers in southern Idaho; Pennsylvanian aquifers along Lake Huron in Michigan; Surficial and Biscayne aquifer systems along Florida's west coast; Northern Atlantic Coastal Plain aquifer system Eastern in New Jersey and New York; Silurian-Devonian aquifers spanning Wisconsin, Illinois and Ohio; and Cambrian-Ordovician aquifer system in parts of Wisconsin and Illinois. Appendix C includes a map of the principal aquifers in the U.S. for reference.

## 4.2 Correlation trends

The correlation coefficients of total dissolved solids, specific conductance, molality, ionic strength, hardness and alkalinity with least work of separation can be found in Table 4.2. Hardness and alkalinity weakly relate to least work of separation, while total dissolved solids, specific conductance, molality and ionic strength strongly relate to least work of separation. We develop simplified equations for least work of separation as a function of recovery ratio and total dissolved solids, specific conductance, molality and ionic strength, all of which have correlation coefficients greater than 0.8. These equations allow for least work of separation estimation based on a chosen groundwater parameter (TDS, specific conductance, molality, ionic strength) and consequently eliminate the need for detailed water composition information required in evaluating the least work from the Pitzer-Kim model.

Table 4.2: Correlation coefficient $R$ of various physical and chemical water properties with least work of separation.

| Parameter | Correlation Coefficient $R$ |
|---|---|
| Alkalinity (mg/L) | 0.28 |
| Hardness (mg/L) | 0.31 |
| Ionic strength (mol/kg) | 0.81 |
| Molality (mol/kg) | 0.99 |
| Specific Conductance ($\mu$S/cm) | 0.95 |
| Total dissolved solids (mg/L) | 0.93 |

### 4.2.1 Total dissolved solids

TDS can be indirectly measured through specific conductance (refer to Appendix F), and feedwater to desalination systems is typically described in terms of TDS. Therefore, establishing a simple equation that calculates the baseline energy requirement for a specified feedwater salinity may prove quite useful for those in the desalination

industry. The correlation coefficient between TDS and least work, 0.93, indicates that these two parameters have a fairly linear relationship, as illustrated in Fig. 4-5. The upper and lower grouping of data in this figure will be explored in Chapter 5.

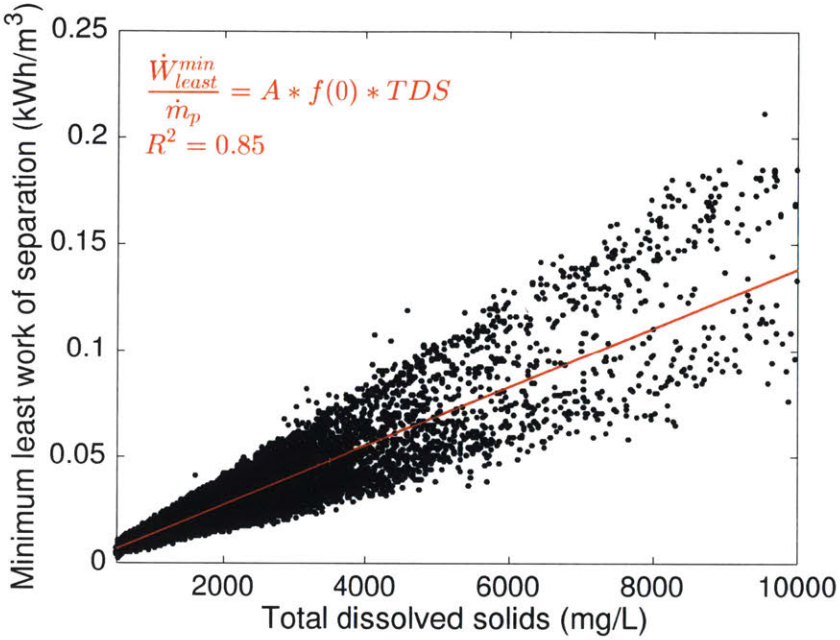


Figure 4-5: Minimum least work of separation as a function of TDS for 28,000 BGW samples with complete composition data. Each dot represents a BGW sample. The best-fit line and its equation, as well as the coefficient of determination, are included in red on the plot. This representation has two separate tails, or trends, occurring above and below the best fit line.

The best-fit line in this figure captures the linearity between TDS and minimum least work of separation, revealing, as expected, that least work increases with increasing TDS. Least work of separation per unit of product can then be written as a function of recovery ratio and total dissolved solids:

$$\frac{\dot{W}_{least}}{\dot{m}_p} = A \times f(r) \times TDS \tag{4.1}$$

where $A$ is a constant equal to 1 (kWh/m$^3$)/(mg/L). The function $f(r)$ is a unitless sixth-order polynomial fit for TDS and least work computed at recoveries ranging

from 0%-90%:

$$f(r) = \sum_{n=0}^{6} a_i r^i \tag{4.2}$$

The polynomial accounts for the increase in least work as a function of recovery ratio; when $r$=0, $f(r) = a_0$, and Eq. (4.1) collapses to the minimum least work. As a result, least work of separation can be evaluated at a recovery $r$ up to 90%. Table 4.3 includes the constants needed to calculate $f(r)$. The relative percent error between least work of separation values calculated using Eqs. (4.1) and (3.3) is determined for each BGW sample. The average error and standard deviation are 20.2% and 15.8%, respectively. The deviation of Eq. (4.1) from actual least work values will increase for samples containing a TDS outside of 500-10,000 mg/L.

Table 4.3: Constants needed to evaluate $f(r)$ for total dissolved solids.

| $i$ | 0 | 1 | 2 | 3 | 4 | 5 | 6 |
|---|---|---|---|---|---|---|---|
| $a_i \times 10^5$ | 1.380 | 0.5576 | 3.196 | −17.23 | 47.94 | −58.71 | 27.75 |

### 4.2.2 Specific conductance

Specific conductance (SC) measures a saline water solution's ability to conduct electricity. Since instrumentation for SC data acquisition is readily available and inexpensive, this parameter can easily be measured in the field with over 95% accuracy [33]. The correlation coefficient between specific conductance and least work of separation, 0.95, reflects the approximately linear relationship between these two parameters. Least work of separation generally increases with specific conductance, as shown in Fig. 4-6.

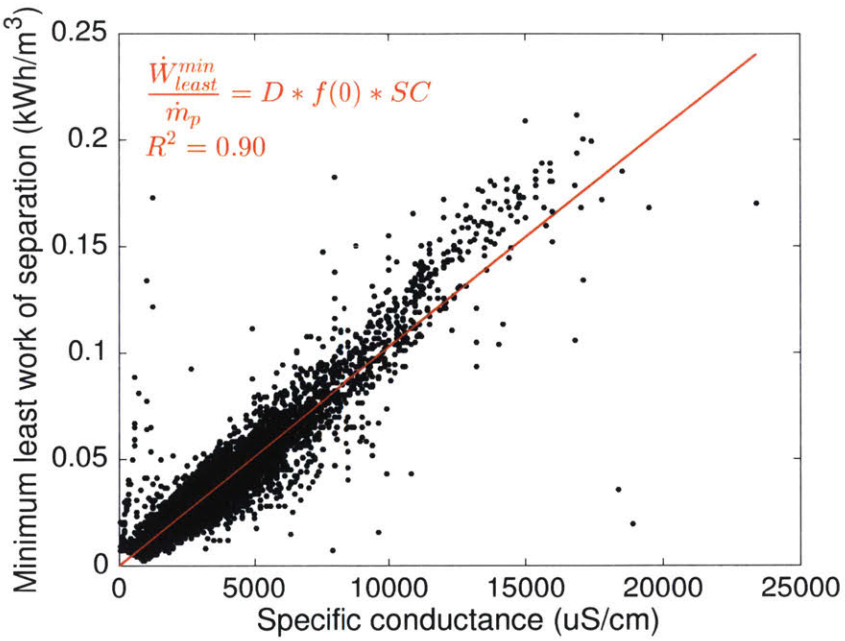


Figure 4-6: Minimum least work of separation as a function of specific conductance for 28,000 BGW samples with complete composition data. Each dot represents a BGW sample. The best-fit line and its equation, as well as the coefficient of determination, are included in red on the plot.

A simplified equation for least work of separation per unit of product can be written as a function of recovery ratio and specific conductance:

$$\frac{\dot{W}_{least}}{\dot{m}_p} = D \times f(r) \times SC \tag{4.3}$$

where $D$ is a constant equal to 1 (kWh/m$^3$)/($\mu$S/cm). The function $f(r)$ is a unitless sixth-order polynomial fit for SC and least work evaluated at recoveries ranging from 0%-90% (see Eq. (4.2)). Table 4.4 includes the constants needed to calculate $f(r)$ for specific conductance. The relative percent error between least work of separation values calculated using Eqs. (4.3) and (3.3) is determined for each BGW sample. The average error and standard deviation are 16.5% and 18.2%, respectively. The divergence of Eq. (4.1) from actual least work values will increase for solutions with a specific conductance outside of 17 - 23,400 $\mu$S/cm. Consequently, in this SC range, least work of separation can be determined with reasonable accuracy with one simple field measurement.

Table 4.4: Constants needed to evaluate $f(r)$ for specific conductance.

| $i$ | 0 | 1 | 2 | 3 | 4 | 5 | 6 |
|---|---|---|---|---|---|---|---|
| $a_i \times 10^6$ | 10.26 | 4.141 | 24.08 | −129.9 | 361.3 | −442.3 | 209.0 |

### 4.2.3 Molality

The correlation coefficient between molality and least work of separation, 0.99, signifies that these two parameters have an almost perfectly linear relationship, corresponding to expected behavior based on the physics outlined in Chapter 3. More specifically, least work is directly related to osmotic pressure, which is a colligative property of mixtures. Colligative properties depend only on the number of moles of solute per unit solution, when solute concentrations are low as in brackish groundwater [34]. Figure 4-7 demonstrates least work of separation grows with increasing molality in a nearly 1:1 manner, lacking the two separate trends seen in Fig. 4-5.

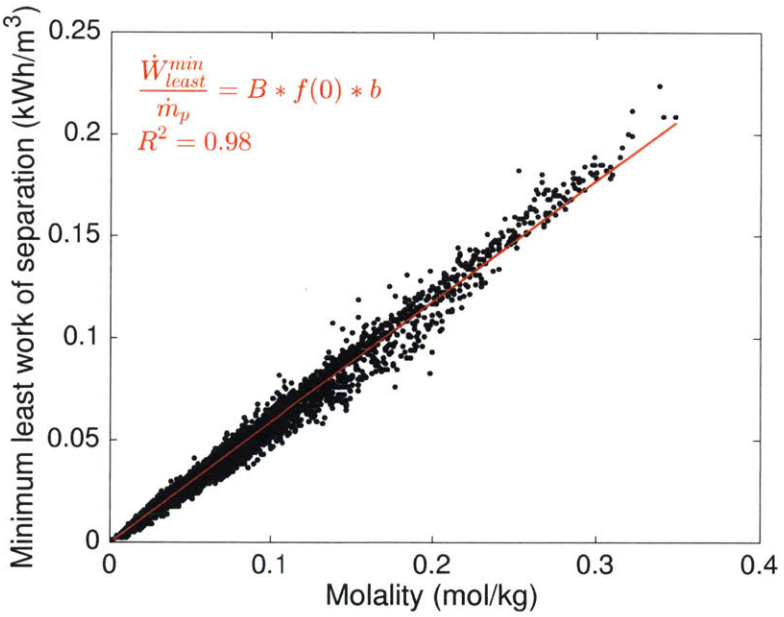


Figure 4-7: Minimum least work of separation as a function of molality for 28,000 BGW samples with complete composition data. Each dot represents a BGW sample. The best-fit line and its equation, as well as the coefficient of determination, are included in red on the plot.

Therefore, least work of separation per unit of product can be determined with solely recovery ratio and feedwater molality:

$$\frac{\dot{W}_{least}}{\dot{m}_p} = B \times f(r) \times b \tag{4.4}$$

where $B$ is a constant equal to 1 (kWh/m$^3$)/(mol/kg). The function $f(r)$ is a unitless sixth-order polynomial fit of best-fit lines for molality and least work computed at recoveries ranging from 0%-90% (see Eq. (4.2)). The constants needed to calculate $f(r)$ are given in Table 4.5. We determine the relative percent error between least work of separation values computed using Eqs. (4.4) and (3.3) for each BGW sample. The average error and standard deviation are 6.31% and 5.66%, respectively, both of which are less than values from the TDS-based and SC-based correlations. The deviation of Eq. (4.4) from actual least work values will increase for samples with a molality outside of 0.0024 - 0.34 mol/kg. Since the correlation coefficient of molality with least work is almost one and the average error is quite low, Eq. 4.4, instead of the Pitzer-Kim model, can be used to calculate the least work of separation with very high accuracy for samples containing 500-10,000 mg/L of TDS.

Table 4.5: Constants needed to evaluate $f(r)$ for molality.

| $i$ | 0 | 1 | 2 | 3 | 4 | 5 | 6 |
|---|---|---|---|---|---|---|---|
| $a_i \times 10^1$ | 5.911 | 2.386 | 13.93 | −75.31 | 209.8 | −257.2 | 121.6 |

### 4.2.4 Ionic strength

Molal ionic strength is defined in terms of the charge $z$ and molality of each ion species [35]:

$$I = \frac{1}{2}\sum_i m_i z_i^2 \tag{4.5}$$

The summation includes all solute ion species $i$ in solution. The correlation coefficient between ionic strength and least work, 0.81, implies that these two variables have a

relatively strong linear dependence on one another, as shown in Fig. 4-8. Although Fig. 4-8 shares a triangular-like shape with Fig. 4-5, ionic strength fans outward from the origin far more than TDS. Figure 4-8 includes a best-fit line, showing that least work of separation increases with ionic strength.

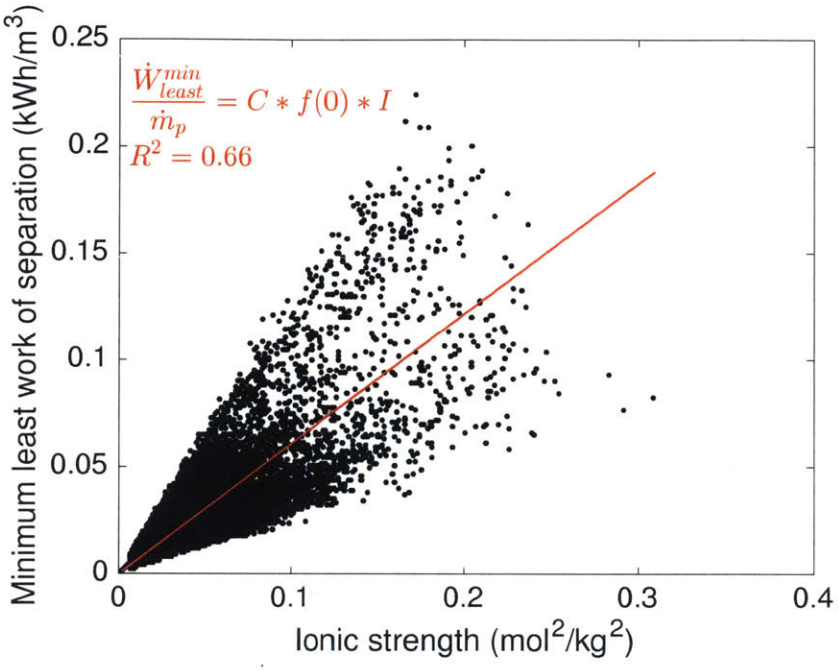


Figure 4-8: Minimum least work of separation as a function of ionic strength for 28,000 BGW samples with complete composition data. Each dot represents a BGW sample. The best-fit line and its equation, as well as the coefficient of determination, are included in red on the plot.

A linearized equation for least work of separation per unit of product in terms of ionic strength and recovery ratio is developed:

$$\frac{\dot{W}_{least}}{\dot{m}_p} = C \times f(r) \times I \tag{4.6}$$

where $C$ is a constant equal to 1 (kWh/m$^3$)/(mol/kg). The function $f(r)$ is a unitless sixth-order polynomial fit of best-fit lines for ionic strength and least work computed at recoveries ranging from 0%-90% (see Eq. (4.2)). Table 4.6 contains the constants necessary for calculating $f(r)$. The relative percent error between least work of separation values from Eqs. (4.6) and (3.3) is evaluated for each BGW sample. The

average error and standard deviation are 30.8% and 23.5%, respectively. The departure of Eq. (4.6) from actual least work of separation will increase for samples with an ionic strength outside of 0.0021 - 0.31 mol/kg.

Table 4.6: Constants needed to evaluate $f(r)$ for ionic strength.

| $i$ | 0 | 1 | 2 | 3 | 4 | 5 | 6 |
|---|---|---|---|---|---|---|---|
| $a_i \times 10^1$ | 3.047 | 1.258 | 6.727 | −36.63 | 102.8 | −126.5 | 60.0 |

# Chapter 5

# Chemical composition

This section examines how groundwater ion composition influences least work of separation. We investigate differences in least work at a fixed TDS by comparing the separation requirements of major ion constituents. We then show the geographic distribution of total dissolved solids, well depth, and major ions across the U.S. Figures illustrate that groundwater composition, which is a principal determinant of least work of separation, varies significantly across the nation. The geographic distribution of saturation indexes and pH across the United States can be found in Appendix D. Appendix E includes additional maps of TDS, well depth and major ions.

## 5.1 Major ions

The dominant cations $C$ in the dataset's groundwater samples are calcium and sodium, while the dominant anions $A$ are bicarbonate, sulfate and chloride. The formation of cation-anion pairs results in six major electrolytes in BGW samples: calcium bicarbonate, calcium sulfate, calcium chloride, sodium bicarbonate, sodium sulfate and sodium chloride. We denote an anion or cation major on a mass basis when it accounts for over 50% of the total mass anion or cation concentration, respectively:

$$\text{major ion} = \frac{m_i}{\sum_{i \in (C \text{ or } A)} m_i} > 0.5 \tag{5.1}$$

Sodium and calcium constitute the major cation in 51% and 25% of BGW samples, respectively. Almost all of the remaining BGW samples contain a combination of sodium and calcium as major cations (i.e., $m_{Na} + m_{Ca} > 0.5\sum_{i\in C} m_i$). Chloride, sulfate and bicarbonate are major anions in 9.0%, 26% and 48% of BGW samples, respectively. The remaining samples contain a combination of the three as dominant anions (i.e., $m_{Cl} + m_{SO_4} + m_{HCO_3} > 0.5\sum_{i\in A} m_i$).

## 5.2 Effect of major ions on least work of separation

Figure 4-5 shows that the TDS-based fit, Eq. (4.1), does not capture the full dependence of Eq. (3.3) on the specific ions in groundwater: two distinct "tails" appear above and below the best-fit line. This separation shows that BGW samples with equal TDS can have different separation requirements. The presence of different sets of constituent ions accounts for this phenomenon. Figure 5-1 is a plot of least work of separation for six single electrolyte solutions containing a TDS of 1,000 mg/L. The six salts shown are the major electrolytes found in BGW samples in the dataset.

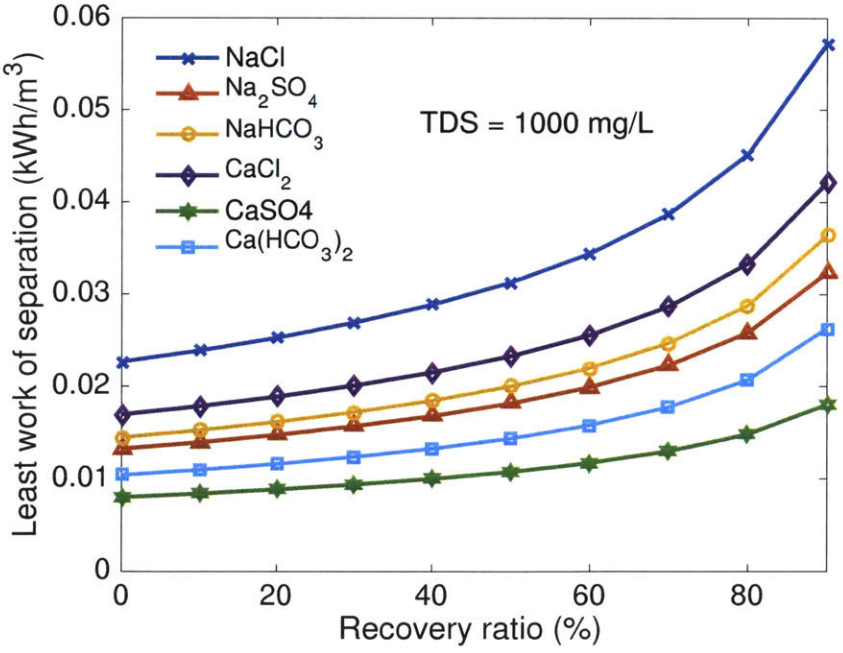


Figure 5-1: Least work of separation for six single electrolyte solutions containing a TDS of 1000 mg/L as a function of recovery ratio ranging from 0%-90%.

Regarding cations, water with sodium tends to require more work to achieve separation than water with calcium at fixed TDS. The general trend among anions is that separation energy decreases in going from chloride to bicarbonate to sulfate. Consequently, heavier electrolytes tend to require a lower least work of separation, partly because of lower molality, increased ion pairing and higher ionic charge (monovalence vs. divalence) [22].

To further investigate compositional effects on the tail formation in Fig. 4-5, we color BGW sample dots based on the major cation or anion present in the sample. Figure 5-2 shows that samples in which sodium is the major cation tend to have higher separation requirements than those for which calcium is the major cation. However, cations do not appear to explain the presence of the two tails.

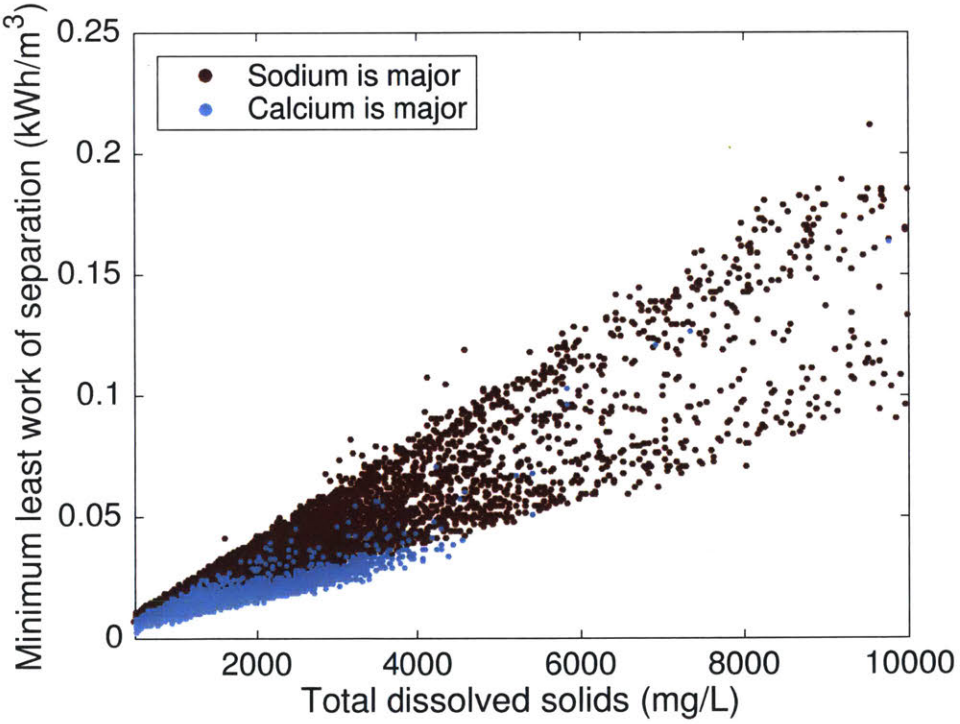


Figure 5-2: Minimum least work of separation as a function of TDS for 28,000 BGW with complete composition data. Each dot corresponds to a BGW sample and is colored based on its major cation, either calcium or sodium, defined in Eq. (5.1).

Figure 5-3 shows that major anions also match the expected trend with chloride, bicarbonate and sulfate in order of decreasing separation requirements. Figure 5-4 shows the same data as Fig. 5-3 without the bicarbonate samples. This figure clearly illustrates that the dominant anions in brackish groundwater solutions result in two distinct trends. BGW samples with chloride as the major anion form the upper tail, while BGW samples with sulfate as the dominant anion form the lower tail. Consequently, anions appear to be the defining factor in least work of separation differences at fixed TDS. Appendix F includes similar plots to those in Figs. 5-2 and 5-3 for specific conductance. Appendix G shows the effect of composition on tail formation in Fig. 4-5 when major cation or anion is defined on a molar basis, rather than a mass basis. The same compositional effects on tail formation occur in both cases.

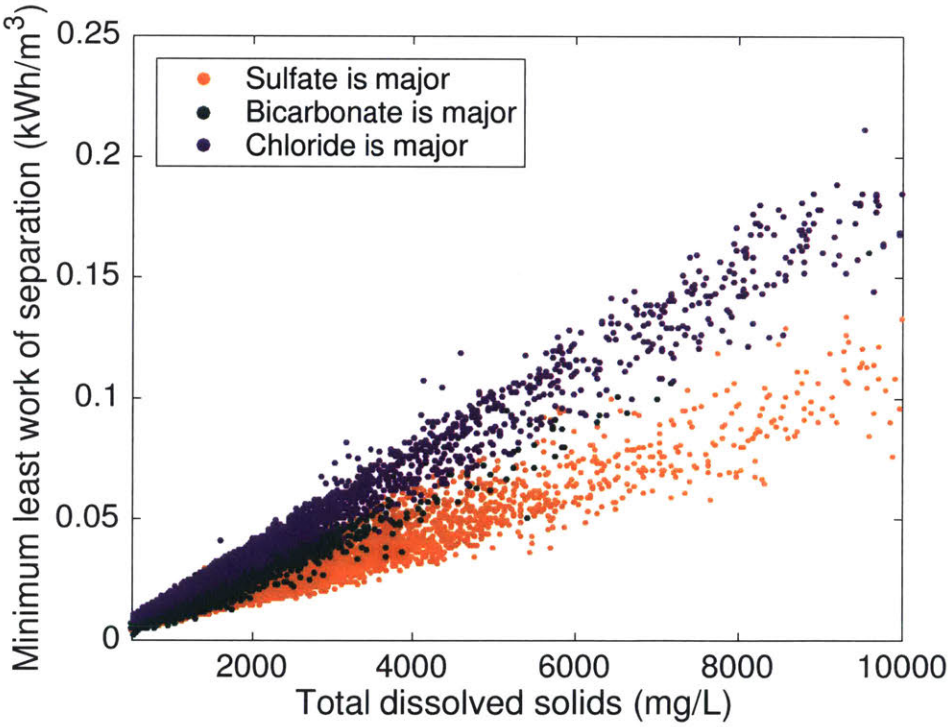


Figure 5-3: Minimum least work of separation as a function of TDS for 28,000 BGW with complete composition data. Each dot corresponds to a BGW sample and is colored based on its major anion, chloride, sulfate or bicarbonate, defined in Eq. (5.1).

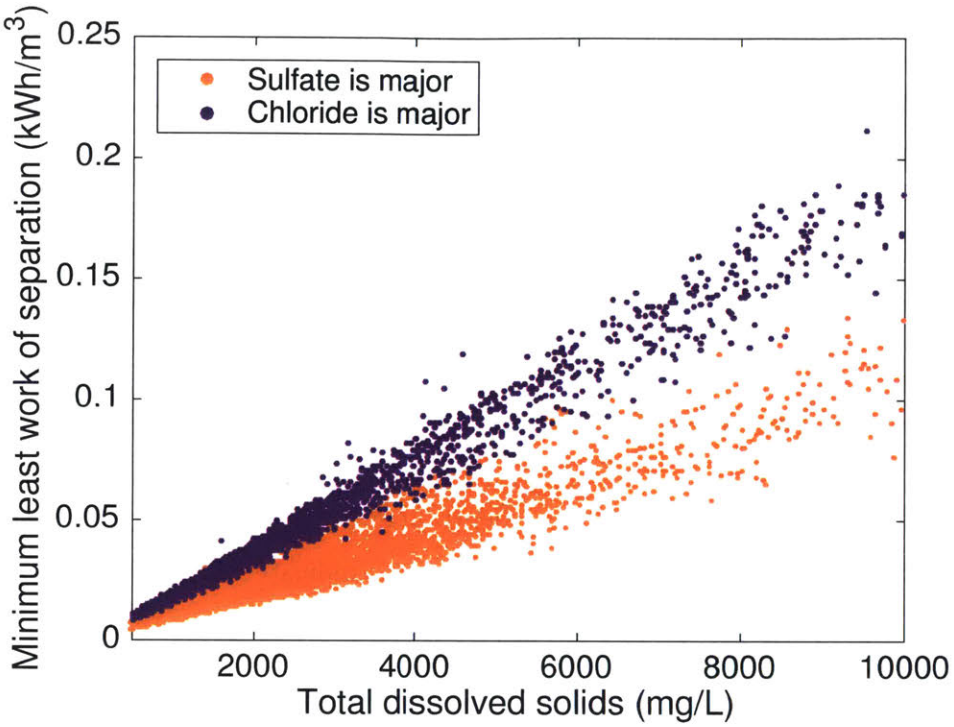


Figure 5-4: Minimum least work of separation as a function of TDS for 28,000 BGW with complete composition data. Each dot corresponds to a BGW sample and is colored based on its major anion, defined in Eq. (5.1). Only chloride and sulfate are included in order to more clearly show tail formation in Fig. 4-5.

## 5.3 Geographic distribution of total dissolved solids, well depth, and major ions

Since least work of separation depends on major ion activities and TDS of a solution, we study the geographic distribution of these parameters across the U.S. TDS and well depth are mapped for 46,000 BGW samples, while major ions are mapped for 28,000 BGW samples that have complete constituent ion data. TDS, major cations and major anions vary considerably across the U.S., similarly to least work. Consequently, location must be taken into account in decision-making regarding site selection for wells. Regions in states and/or principal aquifers containing densely packed groups of TDS or major ions are underscored in order to assist in the resource evaluation process. Appendix C includes a map of the principal aquifers in the U.S. for reference.

The occurrence of clusters highlights composition characteristics that are typically dominant in a given area. As a result, cluster identification will likely prove useful in: 1) determining the most important water parameters to measure when collecting data in the field; 2) estimating desalination energy costs; and 3) minimizing potential membrane scaling in membrane-based desalination systems[1].

### 5.3.1 Total dissolved solids and well depth

Figures 5-5 and 5-6 map TDS and well depth across the continental U.S. Each dot corresponds to a groundwater sample. White areas indicate inadequate data within the USGS dataset. Particularly high densities of groundwater samples occur in the Dakotas, Texas, Central Valley in California and southeastern Kansas. Data representing saline, deeper groundwater was not as accessible. As a result, much of the data included in the maps is biased towards freshwater and shallow resources.

Figure 5-5 illustrates variability of TDS in groundwater across the U.S., in contrast to seawater composition, which remains consistent over larger areas. Approximately 91% of BGW samples contain 500 - 3,000 mg/L TDS, and these samples are present in all parts of the U.S. for which data is available. Clusters of high TDS samples (3,000 - 10,000 mg/L) can be found in Central Valley aquifer system in California; Floridian and Surficial aquifer systems on Florida's west coast; parts of North Dakota; Coastal Plain aquifer system in South Texas; Pecos River Basin alluvial aquifer in West Texas; and Blaine aquifer in the Texas Panhandle. These clusters may partly result from water demand and industry in a given area. For example, California experienced a drought for over 5 years that only recently has diminished, resulting in an increased reliance on its freshwater and brackish groundwater resources in Central Valley [37]. In Texas, the oil and gas industry may largely drive the occurrence and distribution of high salinity groundwater wells, since high salinity water can be used in hydraulic fracturing operations, among other applications [38].

[1]Waters with calcium, magnesium, sulfate, and carbonate have a higher scaling propensity [36].

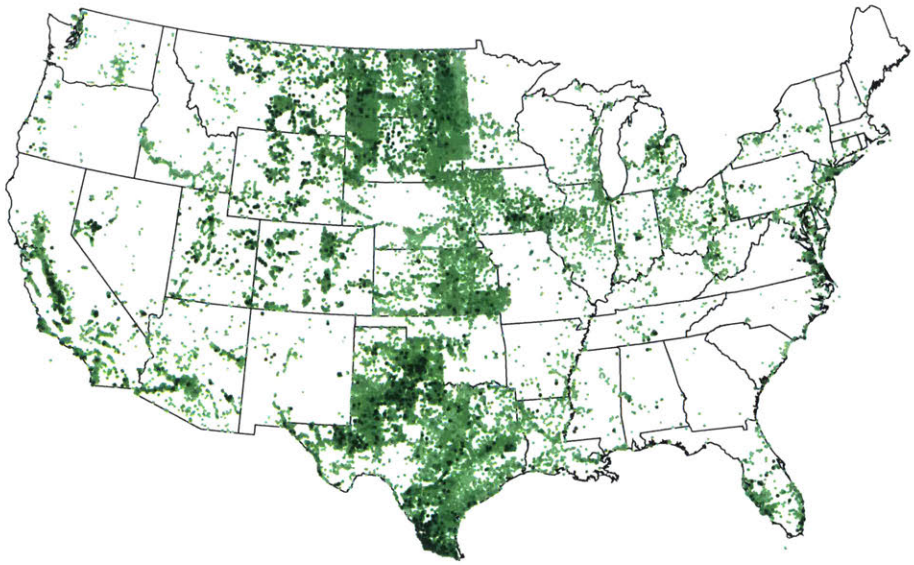

(a)

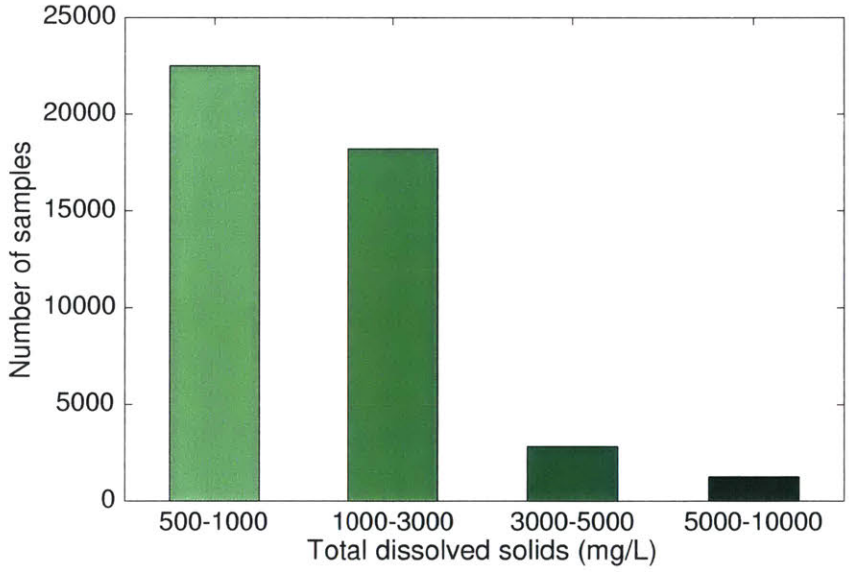


(b)

Figure 5-5: (a) maps total dissolved solids ranging from 500-10,000 mg/L of 46,000 BGW samples across the U.S. Each dot corresponds to a groundwater sample, and each dot color corresponds to one of four TDS brackets, specified in (b). White areas indicate inadequate data. (b) shows the number of samples that fall into each of these brackets.

Since the energy required to desalinate groundwater increases with salinity and well depth (pump lift)[2] [39] , it is useful to understand any correlation between the two. Figure 5-6 maps well depth, measured in meters below the land surface, for BGW samples across the U.S. Approximately 82% of samples have a well depth between 0 - 150 meters. The correlation coefficient between TDS and well depth equals 0.034. This near zero value suggests that deeper groundwater is not necessarily more saline among the samples available. A variety of factors may account for this weak correlation, including seawater intrusion that may raise salinity at shallower well depths along the coasts compared to landlocked regions. As a result, well depth and TDS must be considered independently and in a location-specific manner.

[2]It is important to note that well depth and groundwater table depth are not equivalent. Depending on the aquifer, the pump head may be notably larger than static water table depth due to frictional losses, aquifer depletion, and pressure of water in the aquifer [39]

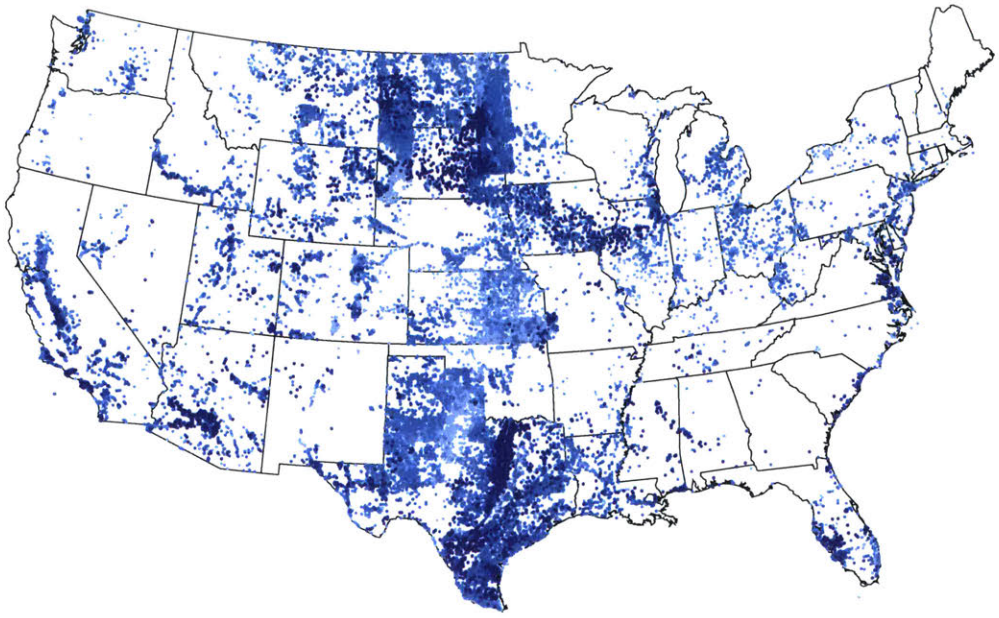

(a)

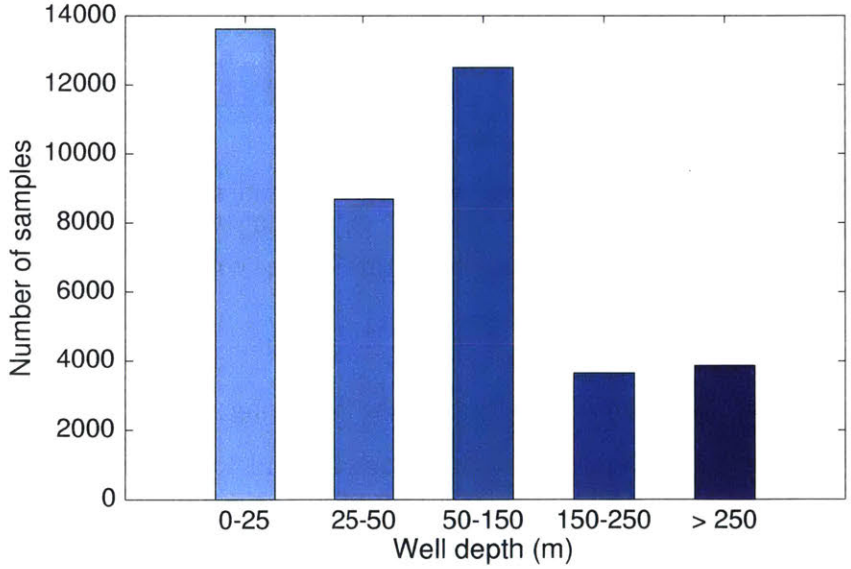


(b)

Figure 5-6: (a) maps well depth ranging from 0-150 meters of 46,000 BGW samples across the U.S. Each dot corresponds to a groundwater sample, and each dot color corresponds to one of five well depth brackets, specified in (b). White areas indicate inadequate data. (b) also shows the number of samples that fall into each of these brackets.

### 5.3.2 Major cations

Figure 5-8 maps major cations across the continental U.S. North Dakota, Texas and California have the largest number of groundwater samples, accounting for the larger number of ion clusters found in these states. Calcium is the major cation in Connecticut, Illinois, Indiana, Iowa, Kansas, Kentucky, Minnesota, Missouri, Nebraska, Ohio, Oklahoma, Pennsylvania, and Wisconsin, while sodium dominates in the remaining states, as can be seen in Fig. 5-7. Despite sodium's prevalence, calcium maintains a considerable presence in almost all states. Major cations appear to be well distributed across states, though the distribution in each state may be non-uniform.

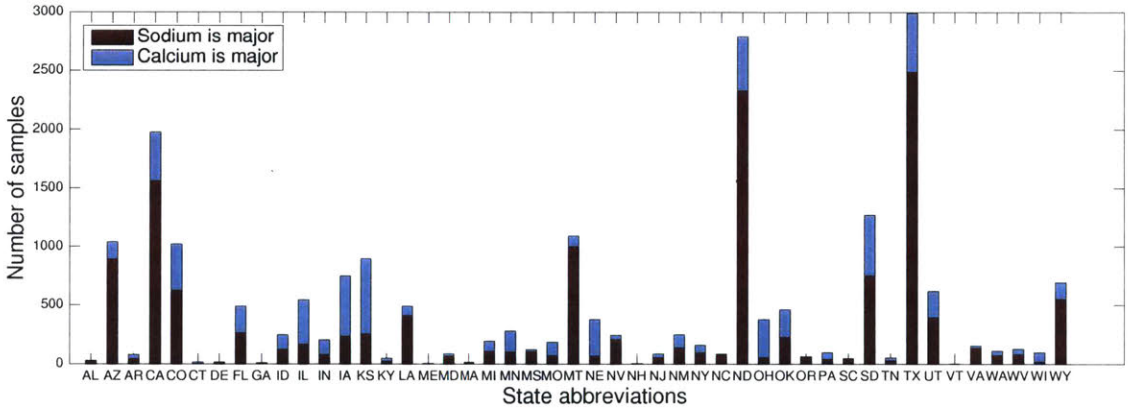


Figure 5-7: Number of BGW samples with calcium and sodium as major cations in each state. Stacked chart includes data for 28,000 BGW samples with complete composition data. Each bar corresponds to a state on the continental U.S. Each color represents a major cation.

Figure 5-8(a) shows calcium clusters in the following inland areas: along the border of the Dakotas and Nebraska with Minnesota and Iowa; parts of Kansas; the Texas Panhandle and south-central Texas; Colorado Plateaus aquifer in north-central Colorado; and Silurian-Devonian aquifers in Illinois and Wisconsin along the Great Lakes. Calcium also appears in some coastal areas: California Coastal Basin aquifer systems along California's southern coast; and Surficial and Biscayne aquifer systems along Florida's west and east coasts.

Some overlap between calcium and sodium exists in the Colorado Plateaus aquifer and the California and Florida coastal regions mentioned above, as can be seen in Fig.

5-8(b). Additional inland areas with groups of sodium ions include Central Valley aquifer system in California; Basin and Range basin-fill aquifers in south-central California and southern Arizona; the Dakotas; Lower Tertiary aquifers in south-central Montana and northern Wyoming; Blaine aquifer in southwestern Oklahoma; Silurian-Devonian aquifers in southeastern Iowa and northwestern Illinois; the Prairies and Lakes region in Texas; and Pennsylvanian aquifers along Lake Huron in Michigan. Additional coastal regions containing sodium clusters are Coastal Plain aquifer systems in South Texas and Louisiana and along the North Atlantic; and Puget Sound aquifer system in northwestern Washington. Sodium's larger presence compared to calcium in coastal areas may partly result from seawater intrusion, although many landlocked regions also contain sodium.

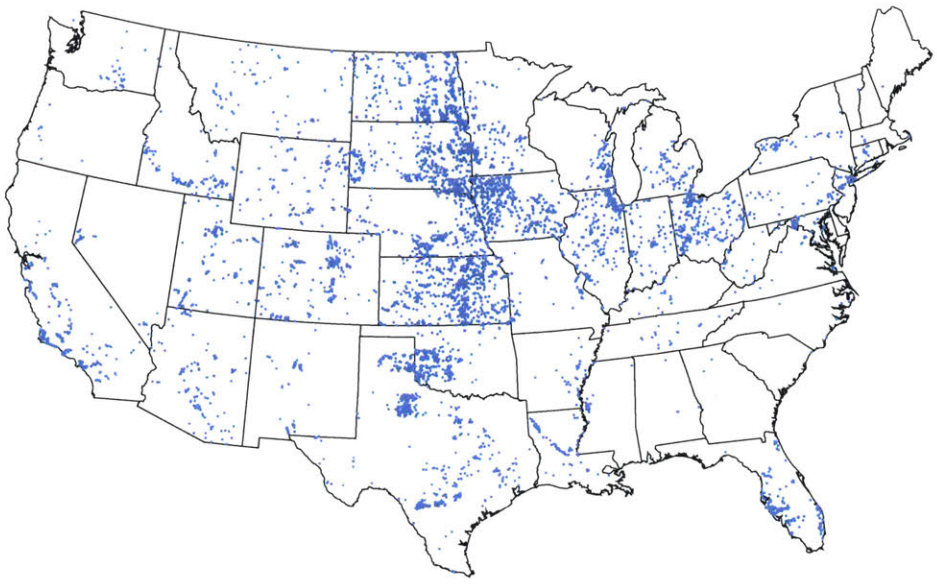

(a)

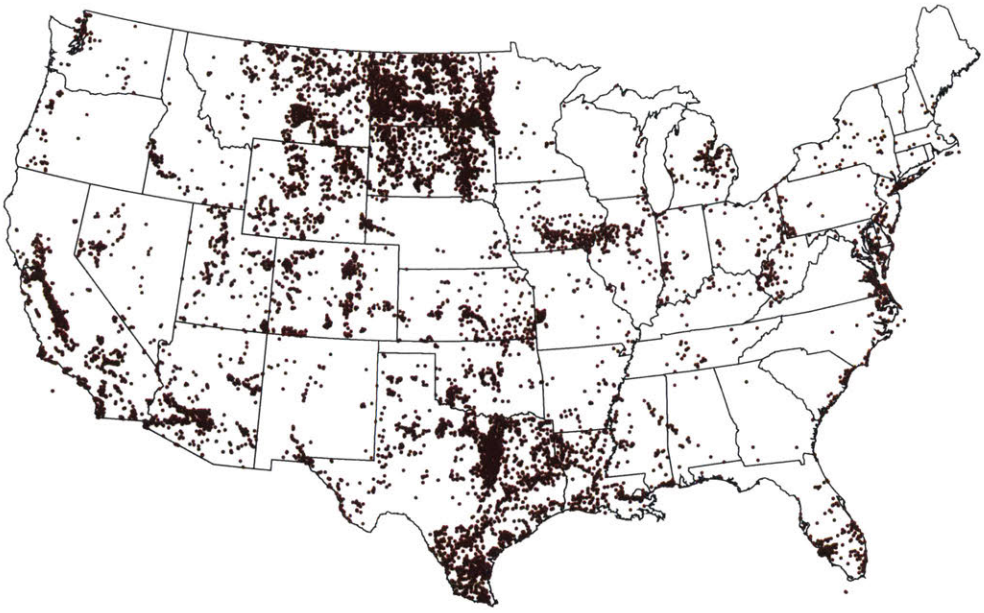

(b)

Figure 5-8: Groundwater samples with (a) calcium and (b) sodium concentrations of greater than 50% total cation concentration are mapped for 28,000 BGW samples with complete composition data. Each dot represents a groundwater sample. White areas indicate a lack of ion composition data.

### 5.3.3 Major anions

Figure 5-10 maps major anions across the continental U.S. North Dakota, Texas, and California have the largest number of groundwater samples, accounting for the larger number of ion clusters found in these states. Figure 5-9 shows that chloride is the dominant anion in Alabama, Arizona, Florida, Massachusetts, New Hampshire, New Jersey and Oregon, sulfate in Colorado, Connecticut, Delaware, Georgia, Montana, South Dakota, Tennessee and Wyoming, and bicarbonate in the remaining states. Despite bicarbonate's prevalence, both chloride and sulfate have considerable presences in California, Texas, Michigan, North Dakota and Utah, and sulfate has sizable occurrences in Arizona, Florida, Iowa, Kansas, New Mexico, Ohio and Oklahoma. Unlike dominant cations, major anions data displays a more uneven distribution across states, in part due to the consideration of three rather than two ions in the anions case.

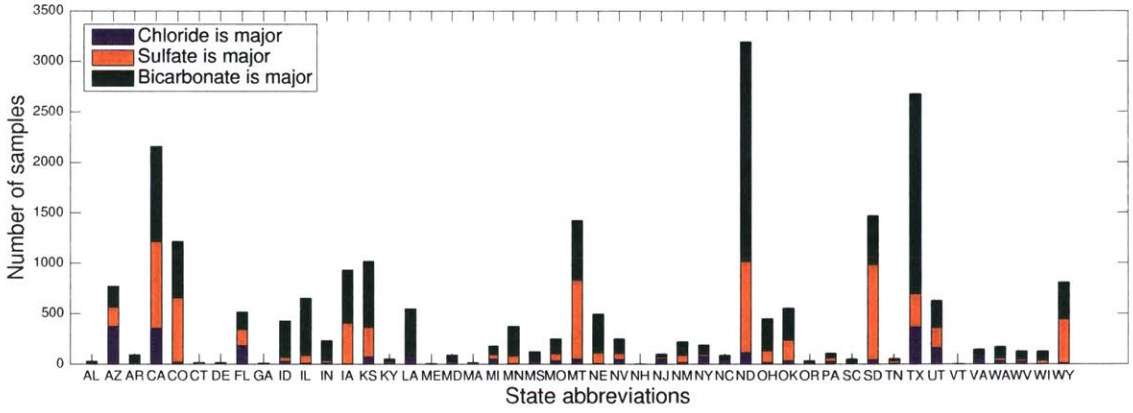


Figure 5-9: Number of BGW samples with chloride, sulfate or bicarbonate as major anion in each state. Stacked chart contains data for 28,000 BGW samples with complete composition data. Each bar corresponds to a state on the continental U.S. Each color represents a major anion.

Chloride is not only restricted to coastal areas, as shown in Fig. 5-10(a). The ion occurs in areas near saline bodies of water, such as Coastal Plain aquifer systems in South Texas and Louisiana and along the North Atlantic; Puget Sound aquifer system in northwestern Washington; Surficial and Biscayne aquifer systems along Florida's west and east coasts; Willamette Lowland basin-fill aquifers near Oregon's west coast;

and Great Salt Lake area in Utah. Chloride is also located in Pennsylvanian aquifers along Lake Huron in Michigan; Basin and Range basin-fill aquifers in south-central California and southern Arizona; parts of North Dakota; and High Plains aquifer in central Kansas.

Bicarbonate occurs as the major anion in many more groundwater samples and many more regions in the U.S. Figure 5-10(b) demonstrates bicarbonate's extensive reach across the nation in almost all coastal and landlocked areas with available BGW data. The USGS data shows that bicarbonate is found in lower TDS solutions. Therefore, a bias towards freshwater also denotes a bias towards bicarbonate samples. Clusters of the anion are located in almost the entire state of North Dakota; Central Valley aquifer system in California; Puget Sound aquifer system in northwestern Washington; Coastal Plain aquifer systems in South Texas and Louisiana and along the North Atlantic; Prairies and Lakes region in Texas; eastern Kansas; Colorado Plateau aquifers in north-central Colorado; Oklahoma's Blaine aquifer and Central Oklahoma aquifer system; Silurian-Devonian aquifers spanning Wisconsin, Illinois, Indiana and Ohio; Surficial and Biscayne aquifer systems along Florida's west and east coasts; and California Coastal Basin aquifer systems along California's southern coast.

Compared to chloride and bicarbonate, sulfate has a larger presence inland relative to coastal across the country, as can be seen in Fig. 5-10(c). In coastal areas, sulfate clusters are situated in Surficial aquifer system along Florida's west coast; and California Coastal Basin aquifer systems along its southern coast. Sulfate-heavy BGW samples are not found along the east coast, northern portion of the west coast or along Texas and Louisiana's coasts, unlike the other anions. Inland, sulfate is located in Central Valley aquifer system and Basin and Range basin-fill aquifers in California; Montana and Wyoming in Lower Tertiary and Upper Cretaceous aquifers; the Dakotas; Colorado Plateaus aquifer in north-central Colorado; Silurian-Devonian aquifer spanning Wisconsin, Illinois, Ohio and Iowa; Mississippian and Lower Cretaceous aquifers in Iowa; Pennsylvanian aquifers in Michigan; Blaine aquifer in southwestern Oklahoma; the Texas Panhandle; and north-central Kansas.

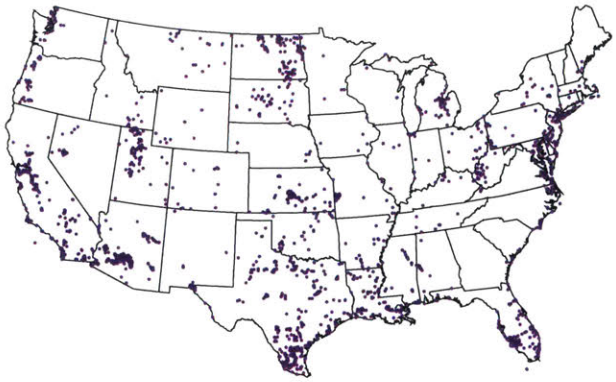

(a)

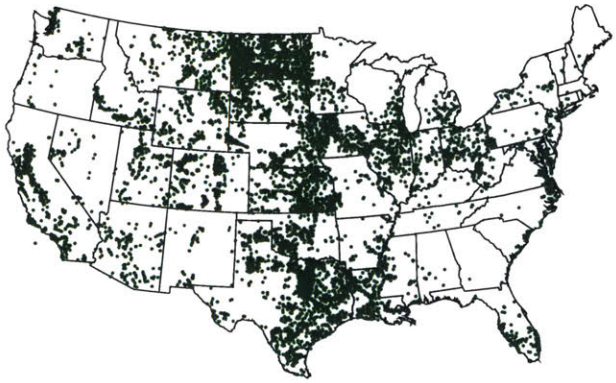

(b)

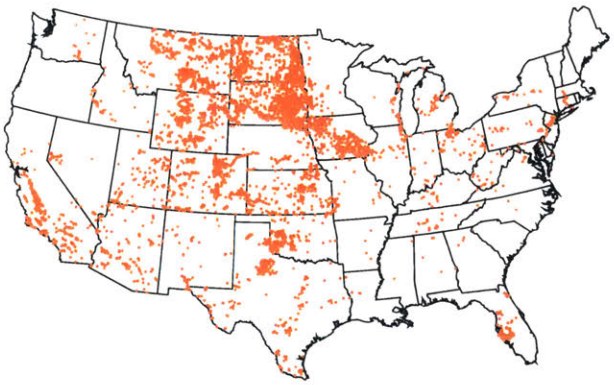

(c)

Figure 5-10: Groundwater samples with (a) chloride, (b) bicarbonate and (c) sulfate concentrations of greater than 50% total anion concentration are mapped for 28,000 BGW samples with complete composition data. Each dot represents a groundwater sample. White areas indicate a lack of ion composition data.

# Chapter 6

# Conclusions

The USGS major-ions dataset for groundwater has been used to assess the minimum work required for desalination of brackish groundwater. The least work of separation has been determined using the Pitzer-Kim mixed electrolyte model. The impact of various groundwater ions has been studied, and several simplified curve fits suitable for use with single-parameter field measurements have been considered. The following conclusions have been reached:

1. Brackish groundwater composition (TDS, major ions) and least work of separation required for brackish groundwater desalination in the U.S. vary considerably across the United States. Therefore, location is an important parameter in decision-making regarding desalination system selection and design.

2. Regions that hold the potential for desalination to reduce the disparity between high water demand and low water supply in a given area can be found throughout the U.S., including parts of California, Arizona, Colorado, North Dakota, South Dakota, Nebraska, Texas, Kansas, Minnesota, Iowa, Oklahoma, Idaho, Michigan, Florida, New Jersey, New York, Wisconsin, Illinois, and Ohio.

3. Simplified equations for least work of separation as a function of total dissolved solids ($R = 0.93$), specific conductance ($R = 0.95$), molality ($R = 0.99$), and ionic strength ($R = 0.81$) are developed. The TDS-based and SC-based correlations enable estimation of least work of separation with one simple field

measurement (SC). These correlations, therefore, eliminate the need for detailed water composition data required for the Pitzer-Kim model. The molality-based correlation can be used to determine the least work of separation with very high accuracy.

4. The major cations in BGW are calcium and sodium, while the major anions are bicarbonate, sulfate and chloride. Sodium is the most commonly dominant cation, while bicarbonate is the most commonly dominant anion. Cluster identification of these ions in states and/or principal aquifers assists in determining the key water parameters in a given area, in estimating desalination energy costs, and in minimizing membrane scaling in membrane-based desalination systems.

5. At a fixed TDS, water with calcium tends to require less work to achieve separation than water with sodium. The general trend among anions is that separation increases in going from sulfate to bicarbonate to chloride.

6. Total dissolved solids and well depth have a very low correlation coefficient of 0.034 among the samples available, indicating that deeper groundwater is not necessarily more saline. Consequently, these parameters must be considered independently and in a location-specific way in the site selection process for groundwater wells.

# Appendix A

# Geochemical sources used in U.S. Geological Survey dataset

U.S. Geological Survey used sixteen geochemical sources to compile the major-ions dataset [14]. These sources range from single publications to large datasets and from state studies to national assessments. USGS was unable to compile all available groundwater data for the nation, particularly from local sources. Instead, the agency relied mainly on larger datasets available in a digital format from state organizations. Table A.1 includes source agency, geographic area in which source agency conducted studies, name of dataset that contains data from studies, and reference for dataset.

Table A.1: Sixteen geochemical sources used by USGS to compile the major-ions dataset.

| Source Agency | Geographic area | Name of dataset | Reference |
|---|---|---|---|
| Arizona Department of Environmental Equality | Arizona | Statewide groundwater quality data | Aiko Condon (Arizona Department of Environmental Quality, written commun., 2013) |
| U.S. Geological Survey | Central Midwest | Central Midwest (RASA Program) | Christi Hansen (U.S. Geolgoical Survey, written commun., 2013) |
| Colorado Department of Agriculture | Colorado | Agricultural chemicals and ground-water protection water quality database | Colorado Department of Agriculture (2013). |
| U.S. Geological Survey, in cooperation with other government and private entities | Colorado | Water-quality data repository | U.S. Geological Survey (2013) |
| Nevada Bureau of Mines and Geology and Great Basin Center for Geothermal Energy | Great Basin | Great Basin groundwater database | Nevada Bureau of Mines and Geology and Great Basin Center for Geothermal Energy (2013). |
| Idaho Department of Water Resources | Idaho | Environmental Data Management System | Idaho Department of Water Resources (2013). |
| Illinois Environmental Protection Agency | Illinois | Water quality data from the Ambient Network of Community Water Supply Wells (CwS Network) | Joe Konczyk (Illinois Environmental Protection Agency, written commun., 2014) |
| Iowa Department of Natural Resources | Iowa | General groundwater quality database of Iowa | Iowa Department of Natural Resources, Geological Survey (2007). |
| Montana Bureau of Mines and Geology | Montana | Geo-Heat Center western states geothermal databases CD | Boyd (2002). |
| New Mexico Bureau of Geology & Mineral Resources | New Mexico | Groundwater monitoring database | Stacy Timmons (New Mexico Bureau of Geology and Mineral Resources, written commun., 2014). |
| New Mexico Interstate Stream Commission Lower Rio Grande Compendium | New Mexico | Groundwater monitoring database | Tom Burley (U.S. Geological Survey, written commun., 2014) |
| Ohio Environmental Protection Agency | Ohio | Ground Water Quality Characterization Program | Ohio Environmental Protection Agency (2013). |
| Texas Water Development Board | Texas | Groundwater database | Texas Water Development Board (2013). |
| U.S. Geological Survey | United States | National geochemical database | Smith (2006). |
| U.S. Geological Survey | United States | National Produced Waters Geochemical Database v2.1 | Blondes and others (2014). |
| U.S. Geological Survey | United States | National Water Information System | U.S. Geological Survey (2016). |

# Appendix B

# Minimum least work of separation

The molar recovery ratio is defined by Eq. (3.6), and the least work of separation can be computed on a molal basis using Eq. (3.5). For a system that desalinates a single electrolyte NaCl solution to produce pure $H_2O$ as product in the limit of infinitesimal extraction (i.e., $\bar{r} \to 0$):

$$\frac{\dot{W}_{least}}{\dot{n}_{H_2O,p}RT} = \cancelto{0}{\left( \ln \frac{a_{H_2O,p}}{a_{H_2O,b}} + b_{NaCl,p} M_{H_2O} \ln \frac{a_{NaCl,p}}{a_{NaCl,b}} \right)}$$

$$-\frac{1}{\bar{r}} \cancelto{0}{\left( \ln \frac{a_{H_2O,f}}{a_{H_2O,b}} + b_{NaCl,f} M_{H_2O} \ln \frac{a_{NaCl,f}}{a_{NaCl,b}} \right)} \tag{B.1}$$

reducing to:

$$\frac{\dot{W}_{least}}{\dot{n}_{H_2O,p}RT} = \ln \frac{a_{H_2O,p}}{a_{H_2O,b}} \tag{B.2}$$

The term in the first set of parentheses limits to zero since $b_{NaCl,p} = 0$ (pure product). The terms in the second set of parentheses represent the change in Gibbs free energy between the feed and brine streams, which approaches zero in the limit of infinitesimal extraction. As a result, the entire term becomes zero divided by zero. The following proof illustrates that it correctly limits to zero:

$$-\frac{1}{\bar{r}} \left( \ln \frac{a_{H_2O,f}}{a_{H_2O,b}} + b_{NaCl,f} M_{H_2O} \ln \frac{a_{NaCl,f}}{a_{s,b}} \right) \stackrel{?}{=} 0 \tag{B.3}$$

Assume ideal behavior for simplicity such that all of the activities in Eq. (B.3) are equivalent to mole fractions $x$:

$$-\frac{1}{\bar{r}}\left(\ln\frac{x_{H_2O,f}}{x_{H_2O,b}}+b_{NaCl,f}M_{H_2O}\ln\frac{x_{s,f}}{x_{s,b}}\right) \tag{B.4}$$

Rewrite molality in terms of mole ratio:

$$b_{NaCl,j}M_{H_2O}=\frac{\dot{n}_{NaCl,j}}{\dot{n}_{H_2O,j}} \tag{B.5}$$

and substitute in the definition of recovery ratio $\bar{r}$ to get:

$$-\frac{\dot{n}_{H_2O,f}}{\dot{n}_{H_2O,p}}\left(\ln\frac{x_{H_2O,f}}{x_{H_2O,b}}+\frac{\dot{n}_{NaCl,f}}{\dot{n}_{H_2O,f}}\ln\frac{x_{s,f}}{x_{s,b}}\right) \tag{B.6}$$

We then set the product flow rate of $H_2O$ equal to $\epsilon$, the brine flow rate of $H_2O$ to $a$, and the equal amount of salt in the feed and brine streams to $b$:

$$\begin{aligned}
&\dot{n}_{H_2O,f}=a+\epsilon \qquad && \dot{n}_{H_2O,b}=a \qquad && \dot{n}_{H_2O,p}=\epsilon\\
&\dot{n}_{NaCl,f}=b \qquad && \dot{n}_{NaCl,b}=b \qquad && \dot{n}_{NaCl,p}=0
\end{aligned}$$

These molar flow rates are used to evaluate the mole fractions $x$:

$$\begin{aligned}
\dot{x}_{H_2O,f}&=\frac{a+\epsilon}{a+b+\epsilon} & \qquad \dot{x}_{H_2O,b}&=\frac{a}{a+b}\\
\dot{x}_{NaCl,f}&=\frac{b}{a+\epsilon+b} & \qquad \dot{x}_{NaCl,b}&=\frac{b}{a+b}
\end{aligned}$$

Substituting the above definitions into Eq. (B.6) yields:

$$-\frac{a+\epsilon}{\epsilon}\left(\ln\frac{\frac{a+\epsilon}{a+b+\epsilon}}{\frac{a}{a+b}}+\frac{b}{a+\epsilon}\ln\frac{\frac{b}{a+b+\epsilon}}{\frac{b}{a+b}}\right) \tag{B.7}$$

which, after simplifying the fraction terms, becomes:

$$-\frac{a+\epsilon}{\epsilon}\left(\ln\frac{1+\frac{\epsilon}{a}}{1+\frac{\epsilon}{a+b}}+\frac{b}{a+\epsilon}\ln\frac{1}{1+\frac{\epsilon}{a+b}}\right) \tag{B.8}$$

Using Taylor expansion on the natural log terms ($\ln(1+\epsilon) \approx \epsilon$, for $\epsilon \ll 1$) gives:

$$= -\frac{a+\epsilon}{\epsilon}\left(\frac{\epsilon}{a} - \frac{\epsilon}{a+b} - \frac{b}{a+\epsilon}\cdot\frac{\epsilon}{a+b}\right) \tag{B.9}$$

Combining fractions results in:

$$= -(a+\epsilon)\left(\frac{(a+b)\epsilon - a\epsilon}{a(a+b)} - \frac{b\epsilon}{(a+\epsilon)(a+b)}\right) \tag{B.10}$$

Assuming $\epsilon \ll a$:

$$= -(a+\epsilon)\left(\frac{b\epsilon}{a(a+b)} - \frac{b\epsilon}{a(a+b)}\right) \tag{B.11}$$

$$= -(a+\epsilon)\left(\frac{b}{a(a+b)} - \frac{b}{a(a+b)}\right)\frac{\epsilon}{\epsilon} \tag{B.12}$$

$$= -a \cdot 0 \cdot 1 = 0 \ \checkmark \tag{B.13}$$

# Appendix C

# Principal aquifers in the United States

A U.S. Geological Survey map of 60 principal aquifers spanning the continental United States is included in Fig. C-1. Each number corresponds to a particular aquifer. Aquifers are colored based on their geologic constitution, since there is a direct relationship between permeability and type of geologic material. The different aquifer categories are: unconsolidated and semi-consolidated sand and gravel aquifers; sandstone aquifers; sandstone and carbonate-rock aquifers; carbonate-rock aquifers; and igneous and metamorphic-rock aquifers. Figure C-1 is then divided into four regions in the U.S (Southwestern Basins, Western Midcontinent, Eastern Midcontinent, Coastal Plains) for clarity in Figs. C-2, C-3, C-4, and C-5.

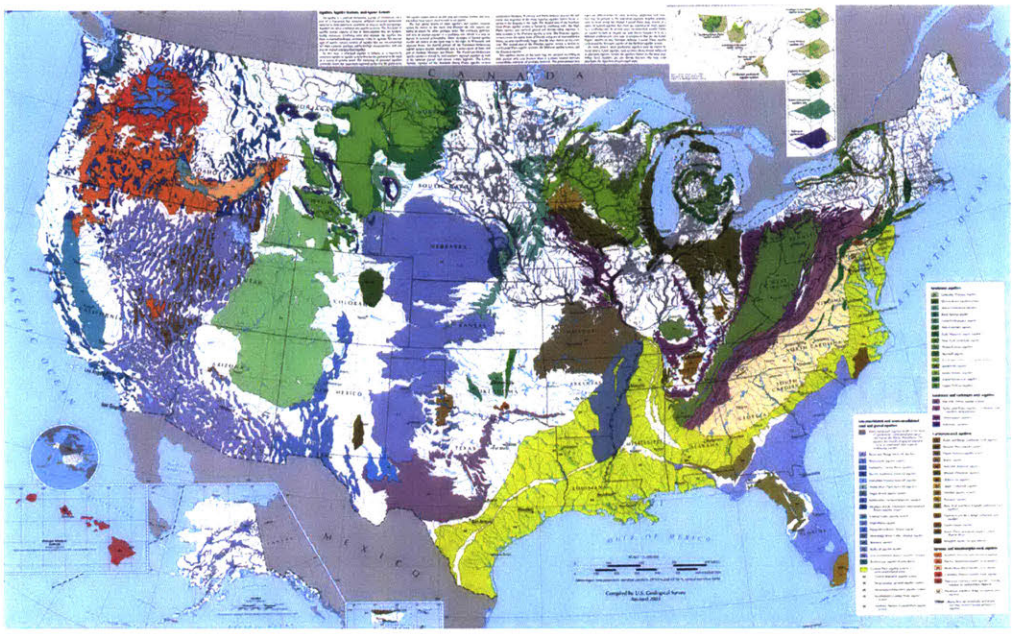

Figure C-1: Map of 60 principal aquifers in the United States [3].

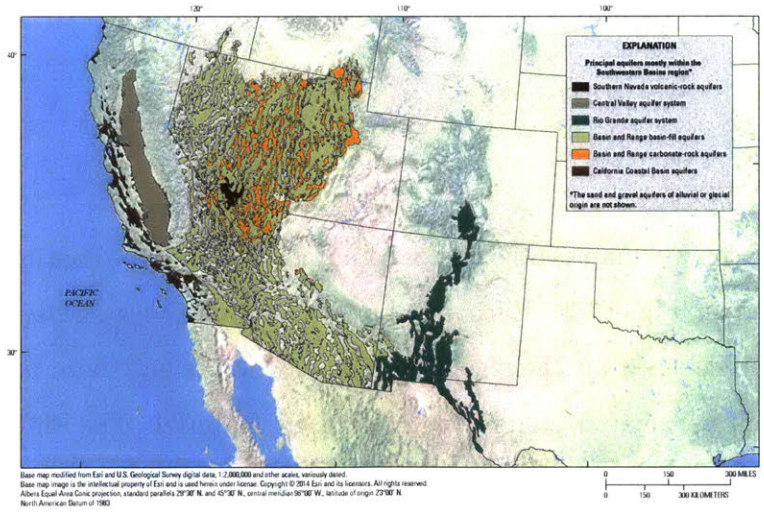


**Figure 35.** Principal aquifers mostly within the Southwestern Basins region.

Figure C-2: Map of principal aquifers within the Southwestern Basins region in the U.S. [3].

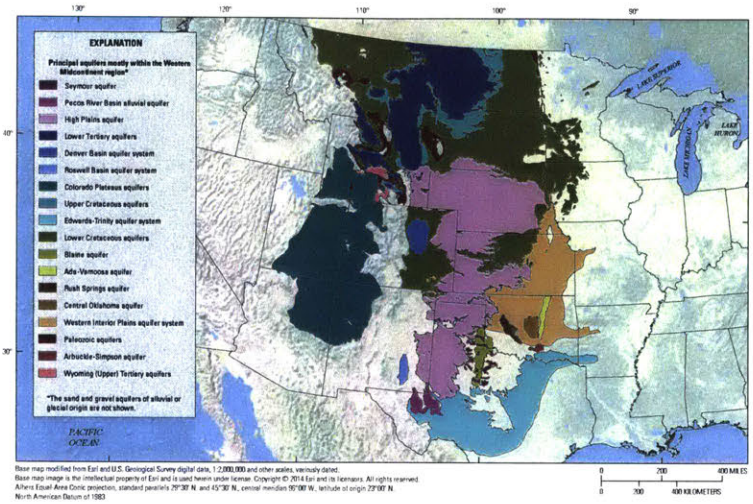


**Figure 41.** Principal aquifers mostly within the Western Midcontinent region.

Figure C-3: Map of principal aquifers within the Western Midcontinent region in the U.S. [3].

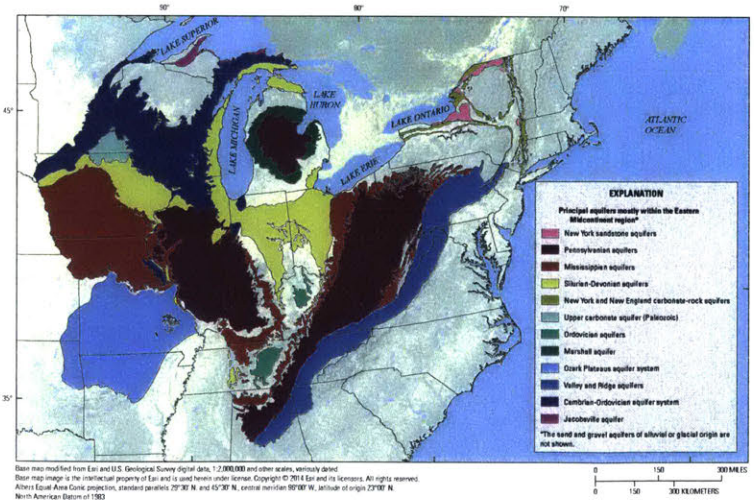


**Figure 27.** Principal aquifers mostly within the Eastern Midcontinent region.

Figure C-4: Map of principal aquifers within the Eastern Midcontinent in the U.S. [3].

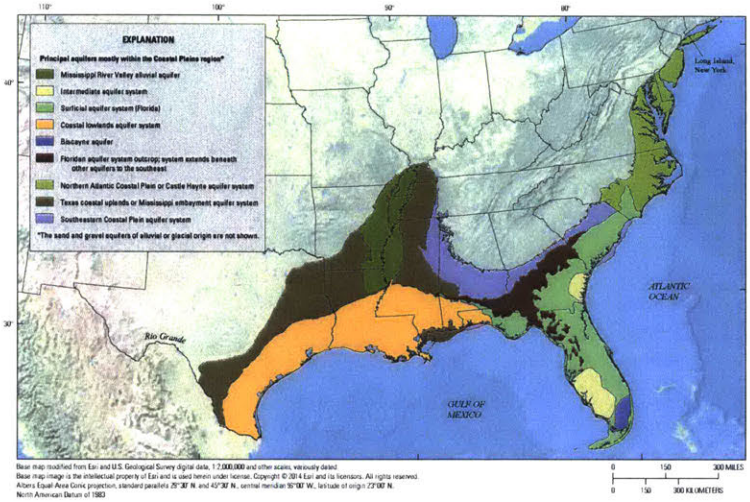


**Figure 21.** Principal aquifers mostly within the Coastal Plains region.

Figure C-5: Map of principal aquifers in the Coastal Plains region of the U.S. [3].

# Appendix D

# Geographic distribution of additional groundwater composition characteristics: saturation index and pH

## D.1 Saturation index

The saturation index (SI) is a commonly used metric for quantifying the occurrence of salt crystallization in a mixture [40]:

$$\mathrm{SI} = \log\left(\frac{Q}{K_{sp}}\right) = \log\left(\frac{a_M^{\nu_M} a_X^{\nu_X} a_w^{\nu_w}}{K_{sp}}\right) \tag{D.1}$$

where $Q$ is the activity product and $K_{sp}$ is the solubility product. Solutions with SI $< 0$ are subsaturated, indicating that any solid phase salts tend to dissolve. Solutions with SI $> 0$ are supersaturated, indicating that any solid phase salts tend to crystallize. Consequently, the saturation index can be used to measure the potential of scale formation on membranes in desalination systems. When SI $<$ -1, the solution can be used as feedwater in desalination systems operating at up to approximately

90% recovery without causing salt crystallization[1]. Brackish water reverse osmosis (BWRO) plants typically operate at recoveries ranging from 75%-90% [31]. Figure D-1 shows the calcite and gypsum saturation indexes of the 28,000 brackish groundwater samples for which least work of separation is calculated in this thesis.

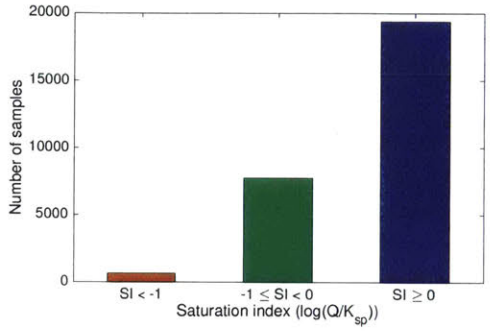


(a)

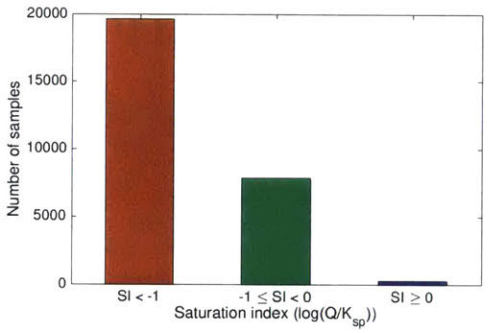


(b)

Figure D-1: Calcite (a) and gypsum (b) saturation index for 28,000 BGW samples.

Approximately 2.3% have a calcite saturation index less than -1, while 70.7% have a gypsum saturation index less than -1. These samples may be used as feedwater in high recovery BWRO systems without calcium carbonate and/or calcium sulfate scale formation. BGW solutions with SI greater than -1 will require pretreatment to prevent scaling in the desalination process. Figures D-2 and D-3 map calcite and gypsum SI, respectively, for the ranges specified in Fig. D-1.

[1]SI < -1 limit is approximate. At SI = $\log \frac{a_{solute}}{K_{sp}} = -1$, the activity of the solute is 10 times less than its activity at its solubility limit. If the activity coefficient does not change, then the concentration would also be 10 times less than at its solubility limit. At a recovery of 90%, the concentration factor CF = $\frac{1}{1-r} = 10$. Therefore, when the activity coefficient does not change as the solute concentration increases, SI = -1 at the beginning of the process corresponds to SI = 0 at the end of the (90% recovery) process. In reality, the activity does increase with concentration.

(a)

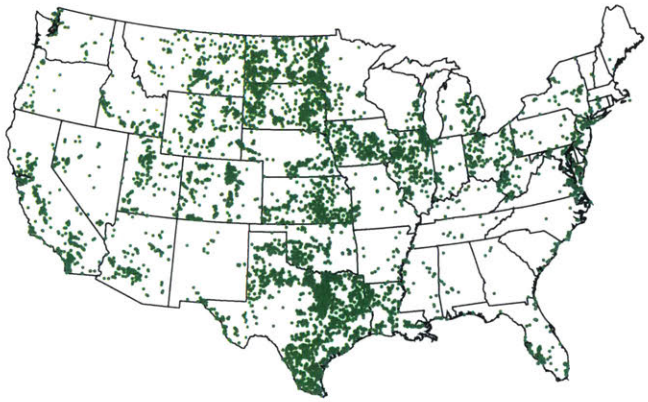

(b)

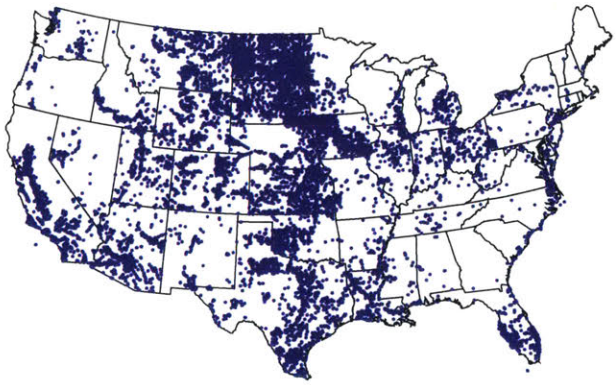

(c)

Figure D-2: Map of calcite saturation index for 28,000 BGW samples (a) SI $< -1$, (b) $-1 \leq$ SI $< 0$, and (c) SI $\geq 0$. Each dot corresponds to a groundwater sample. White areas indicate inadequate data.

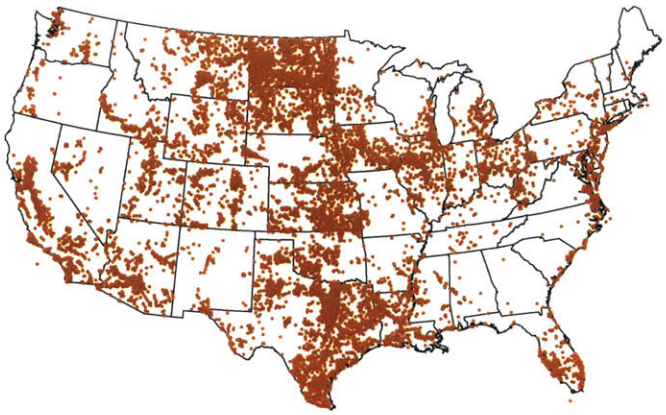

(a)

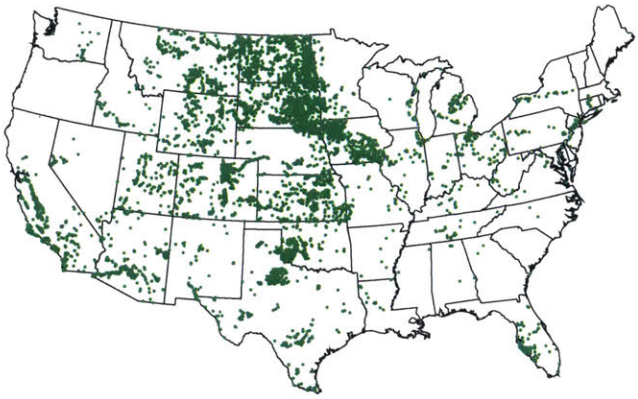

(b)

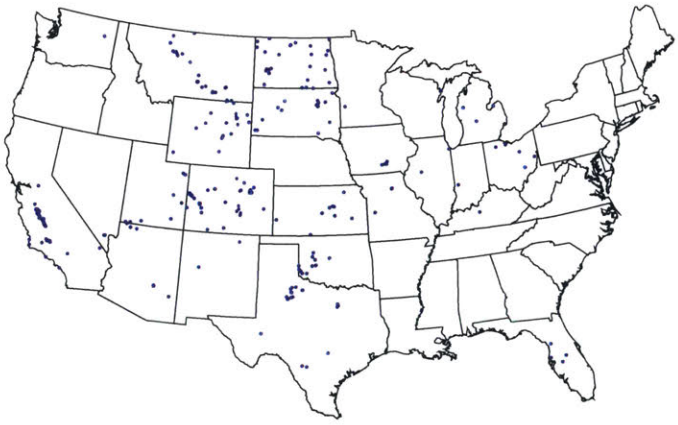

(c)

Figure D-3: Map of gypsum saturation index for 28,000 BGW samples for (a) SI $< -1$, (b) $-1 \leq$ SI $< 0$, and (c) SI $\geq 0$. Each dot corresponds to a groundwater sample. White areas indicate inadequate data.

## D.2 pH

Figure D-4 includes the geographic distribution of pH for the ranges specified in Fig. D-5. The average pH for 28,000 BGW samples with complete composition data is 7.57. The maximum and minimum pH values are 10.5 and 4.1, respectively. Approximately 65% of samples have a pH between 7 and 8, as can be seen in Fig. D-4.

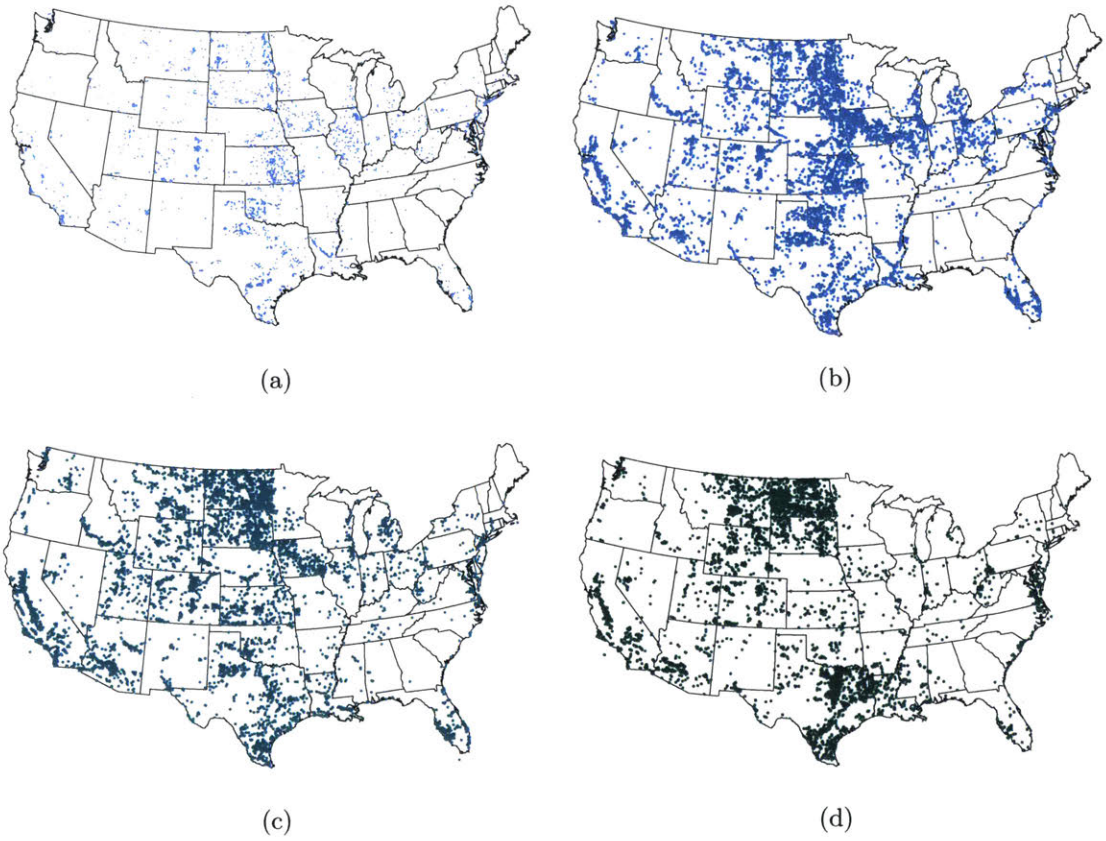

(a) (b)

(c) (d)

Figure D-4: Map of pH for 28,000 BGW samples for (a) pH $< 7$, (b) $7 \leq$ pH $< 7.5$, (c) $7.5 \leq$ pH $< 8$, and (d) pH $\geq 8$. Each dot corresponds to a groundwater sample. White areas indicate inadequate data.

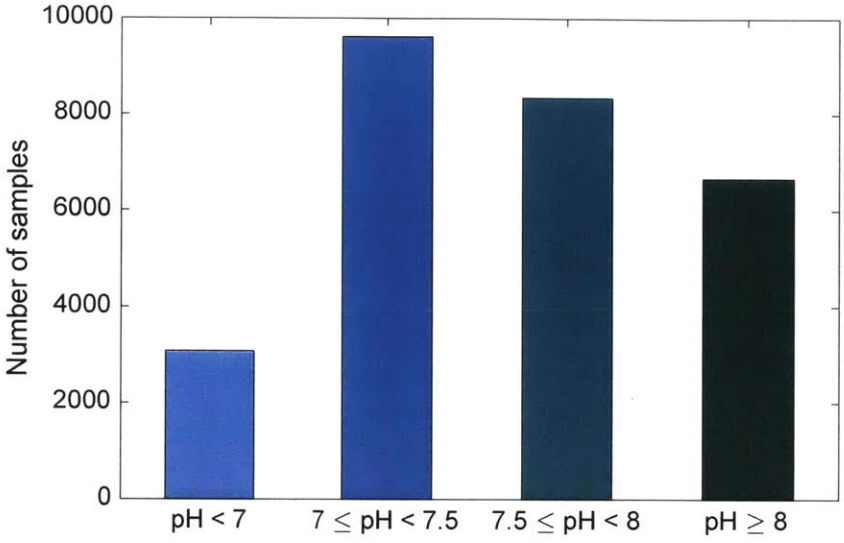


Figure D-5: pH for 28,000 BGW samples.

# Appendix E

# Maps of minimum least work of separation, desalination potential, total dissolved solids, and well depth

Figures below include additional maps of minimum least work of separation, desalination potential, total dissolved solids, and well depth to further elucidate these characteristics' geographic distribution. In Chapters 4 and 5, all brackets of a given parameter were mapped on the same figure. In this section, each bracket is mapped separately. Desalination potential and total dissolved solids sections also include the original maps presented in Chapters 4 and 5 with major rivers and lakes.

## E.1 Minimum least work of separation

Figures E-1, E-2, E-3, E-4, and E-5 show that least work of separation varies considerably across the United States. Approximately 66% of BGW samples have low separation requirements (i.e., $\dot{W}_{least}^{min} = 0 - 0.02$ kWh/m$^3$). They can be found in the following areas: Central Valley in California; Dakotas; southwestern Arizona; Texas; Louisiana; Colorado; Kansas; Nebraska; Idaho; Iowa; Illinois; Florida's west coast; and along the East Coast. Approximately 17% of BGW samples have high separation requirements (i.e., $\dot{W}_{least}^{min} > 0.03$ kWh/m$^3$). They can be found in the following

areas: Central Valley in California; Dakotas; Montana; southern Texas; southwestern Arizona; Florida's west coast; and the East Coast.

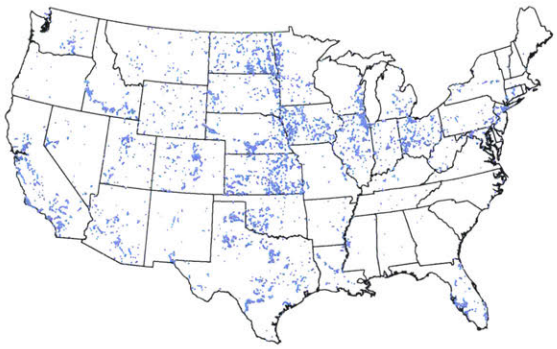

Figure E-1: Map of minimum least work of separation from 0 - 0.01 kWh/m$^3$.

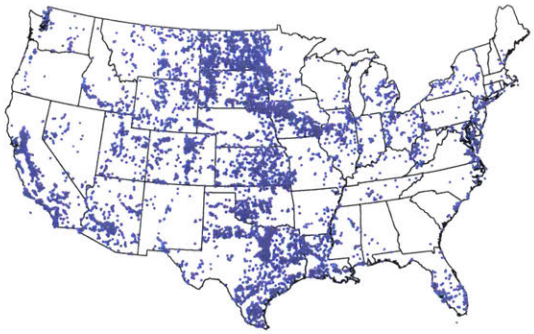

Figure E-2: Map of minimum least work of separation from 0.01 - 0.02 kWh/m$^3$.

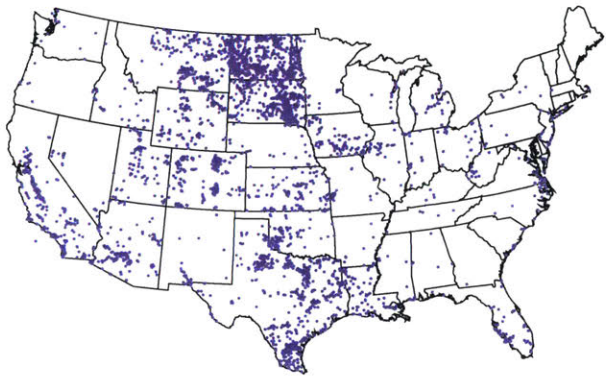

Figure E-3: Map of minimum least work of separation from 0.02 - 0.03 kWh/m$^3$.

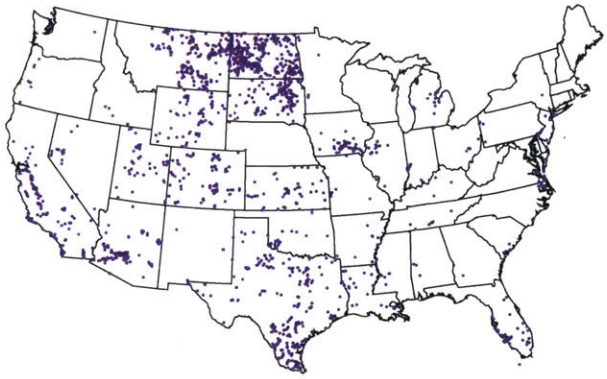

Figure E-4: Map of minimum least work of separation from 0.03 -0.04 kWh/m$^3$.

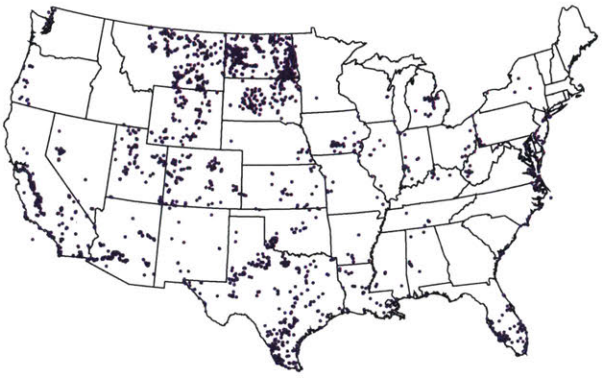

Figure E-5: Map of minimum least work of separation greater than 0.04 kWh/m$^3$.

## E.2 Desalination potential

Figure E-6: Map of samples with minimum least work of separation from 0 - 0.01 kWh/m$^3$ and in high water stress areas.

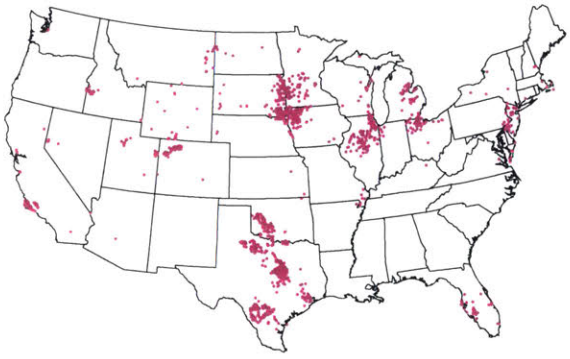

Figure E-7: Map of samples with minimum least work of separation from 0 - 0.01 kWh/m$^3$ and in extremely high water stress areas.

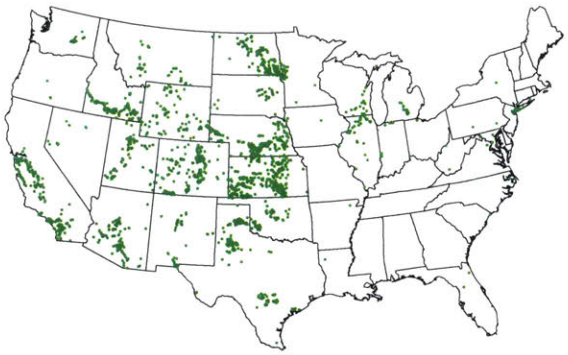

Figure E-8: Map of samples with minimum least work of separation from 0.01 - 0.02 $kWh/m^3$ and in high water stress areas.

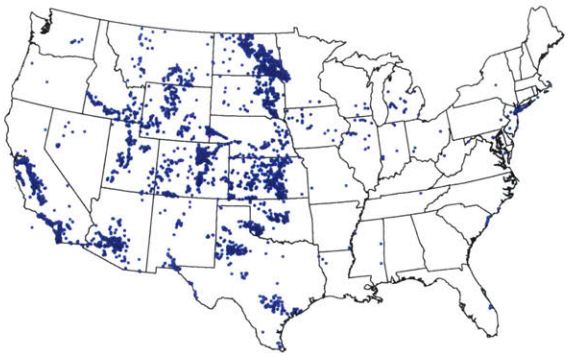

Figure E-9: Map of samples with minimum least work of separation from 0.01 - 0.02 $kWh/m^3$ and in extremely high water stress areas.

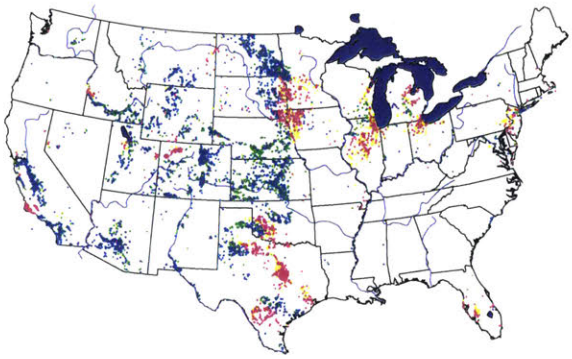

Figure E-10: Map with major rivers and lakes near the groundwater samples that have low least work of separation and high water stress. Rivers may play a role in location of water demand, i.e., increased water stress, since there tends to be higher population densities near rivers. Rivers may also contribute to low salinity supply, i.e., low least work of separation, in surrounding areas due to freshwater intrusion.

## E.3 Total dissolved solids

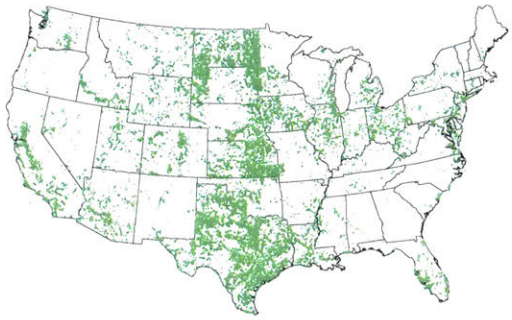

Figure E-11: Map of samples containing 500 - 1,000 mg/L of total dissolved solids.

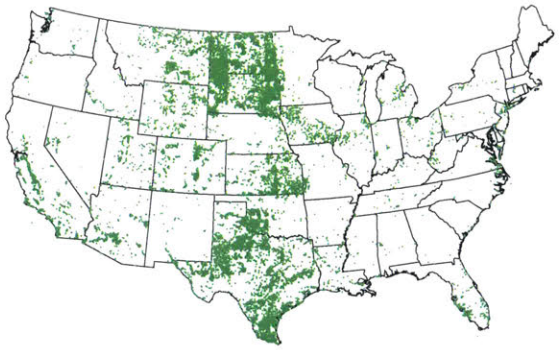

Figure E-12: Map of samples containing 1,000 - 3,000 mg/L of total dissolved solids.

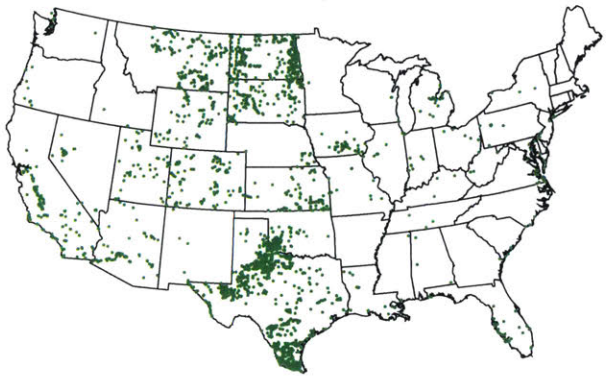

Figure E-13: Map of samples containing 3,000 - 5,000 mg/L of total dissolved solids.

Figure E-14: Map of samples containing 5,000 - 10,000 mg/L of total dissolved solids.

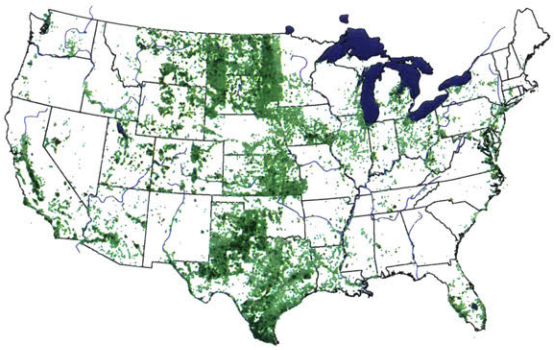

Figure E-15: Map with major rivers and lakes shown along with total dissolved solids of the groundwater samples. Rivers may result in freshwater intrusion and therefore, lower TDS in surrounding areas.

## E.4 Well depth

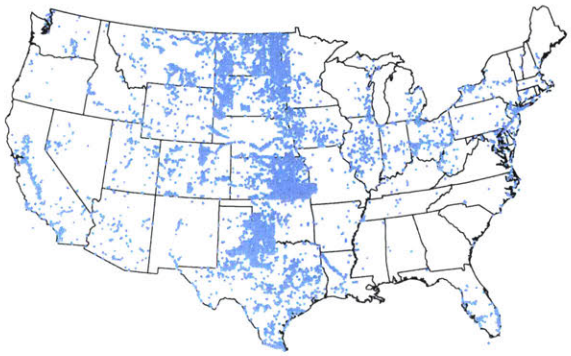

Figure E-16: Map of wells with depth from 0 - 25 meters.

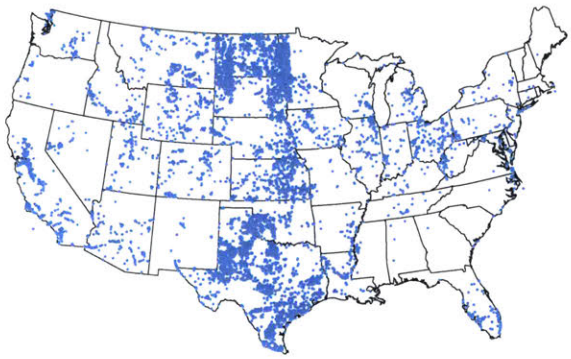

Figure E-17: Map of wells with depth from 25 - 50 meters.

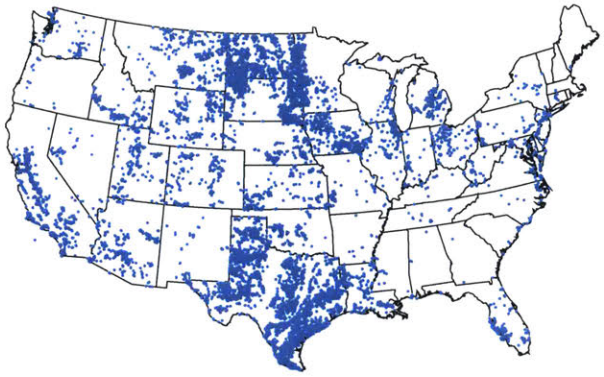

Figure E-18: Map of wells with depth from 50 - 150 meters.

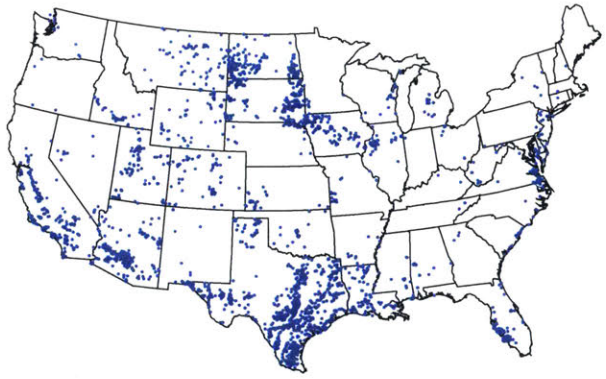

Figure E-19: Map of wells with depth from 150 - 250 meters.

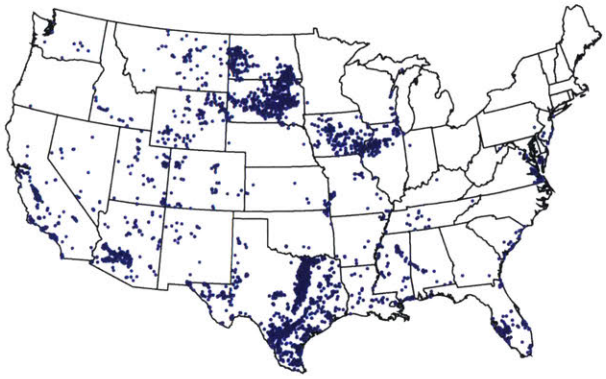

Figure E-20: Map of wells with depth greater than 250 meters.

# Appendix F

# Specific conductance

## F.1 Effect of major ions on specific conductance

To show compositional effects on specific conductance in Fig. 4-6, we color BGW sample dots based on the major cation or anion present in the sample, as defined in Eq. (5.1). Figures F-1, F-2, and F-3 confirm expected trends. Water with sodium tends to require more work to achieve separation than water with calcium. Water with chloride tends to require more work to achieve separation than water with sulfate.

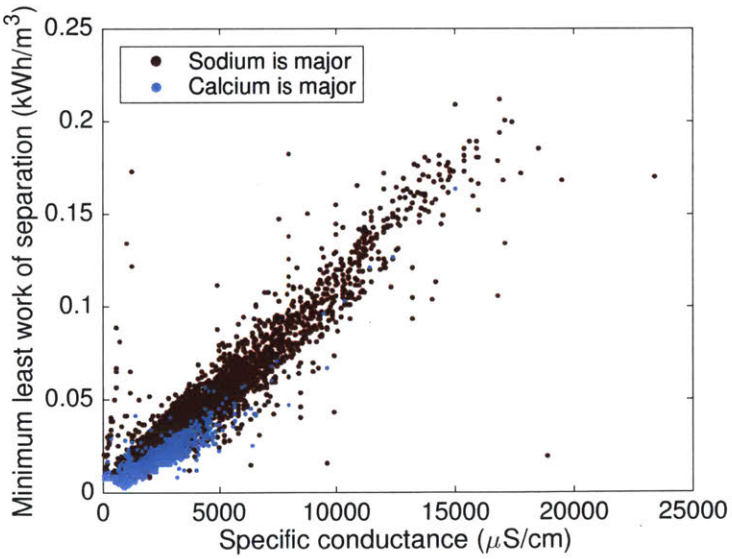


Figure F-1: Minimum least work of separation as a function of SC for 28,000 BGW with complete composition data. Each dot corresponds to a BGW sample and is colored based on its major cation, either calcium or sodium, defined in Eq. (5.1).

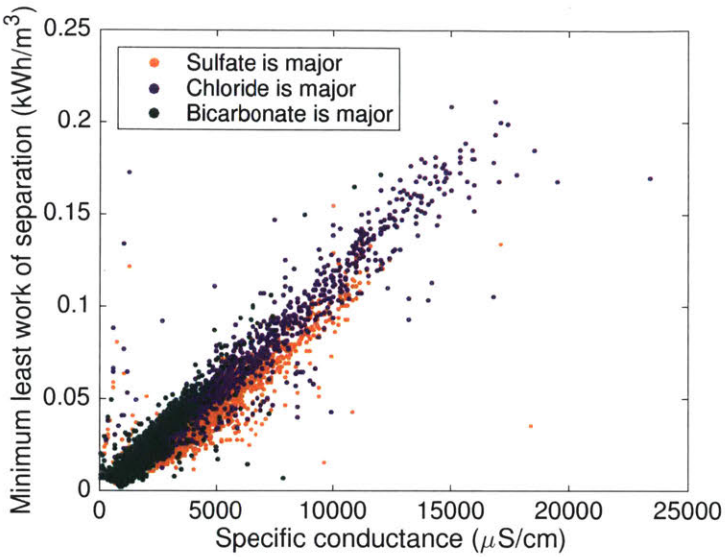


Figure F-2: Minimum least work of separation as a function of SC for 28,000 BGW with complete composition data. Each dot corresponds to a BGW sample and is colored based on its major anion, chloride, bicarbonate or sulfate, defined in Eq. (5.1).

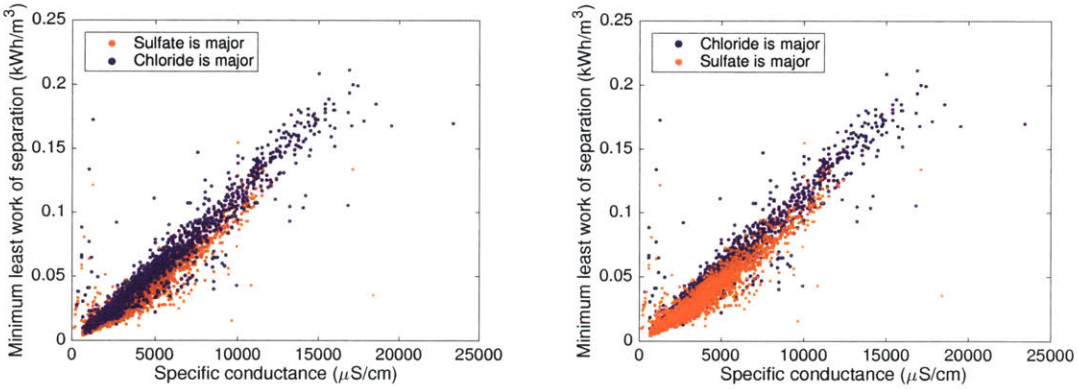


Figure F-3: Minimum least work of separation as a function of SC for 28,000 BGW with complete composition data. Each dot corresponds to a BGW sample and is colored based on its major anion, chloride or sulfate, defined in Eq. (5.1).

## F.2 Conversion from specific conductance to total dissolved solids

Total dissolved solids was reported for over half of the groundwater samples in the USGS dataset, either from the summation of individual constituent concentrations or an analysis of residue after evaporation. For samples lacking these values, specific conductance was converted to total dissolved solids using correlations developed by USGS [3] for SC $< 50,000$ $\mu$S/cm at 25 °C ($R^2 = 0.94$):

$$\text{TDS} = -55 + 0.689 \times \text{SC} \tag{F.1}$$

and for SC $> 50,000$ $\mu$S/cm ($R^2 = 0.92$):

$$\text{TDS} = -27,720 - 0.0869 \times \text{SC} + 6.204 \times 10^{-6} \times \text{SC}^2 \tag{F.2}$$

For low specific conductance values (SC $< 300$ $\mu$S/cm), Eq. (F.1) becomes less reliable. Uncertainties associated with Eqs. (F.1) and (F.2) are caused by data quality and differences in the theoretical relationship between SC and TDS for water with equal TDS but varying ion composition.

# Appendix G

# Effect of major ions defined on a molar basis on least work of separation

In Chapter 5, we define an anion or cation as major on a mass basis in order to explore compositional effects on least work of separation. In this section, we color BGW sample dots based on the major cation or anion present in the sample, defined on a molar basis. An anion or cation is major on a molar basis when it accounts for over 50% of the total molar anion or cation concentration, respectively:

$$\text{major ion} = \frac{b_i}{\sum_{i \in (C \text{ or } A)} b_i} > 0.5 \tag{G.1}$$

The same compositional trends occur when defining major ion on a molar basis, shown in Figs. G-1, G-2 and G-3, as on a mass basis, shown in Figs. 5-2 and 5-3.

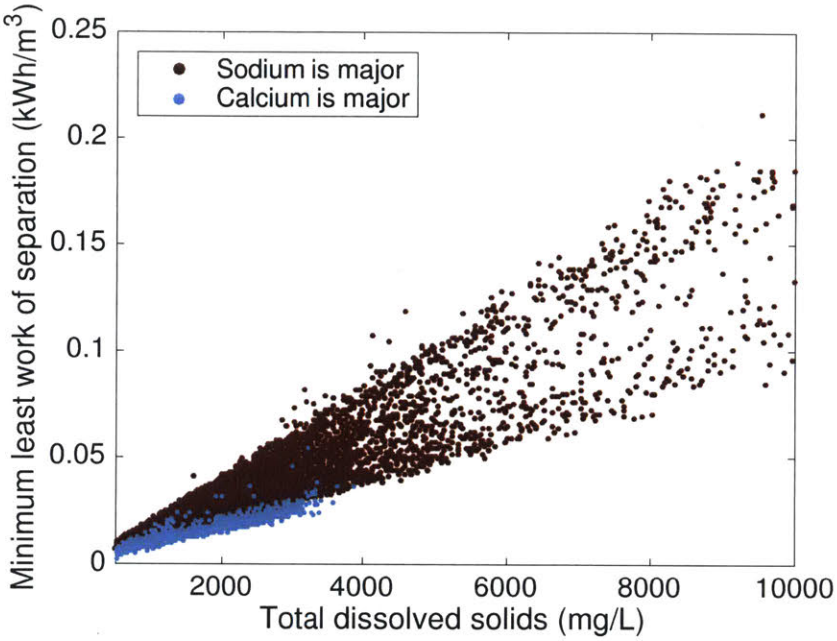


Figure G-1: Minimum least work of separation as a function of TDS for 28,000 BGW with complete composition data. Each dot corresponds to a BGW sample and is colored based on its major cation, either calcium or sodium, defined in Eq. (G.1).

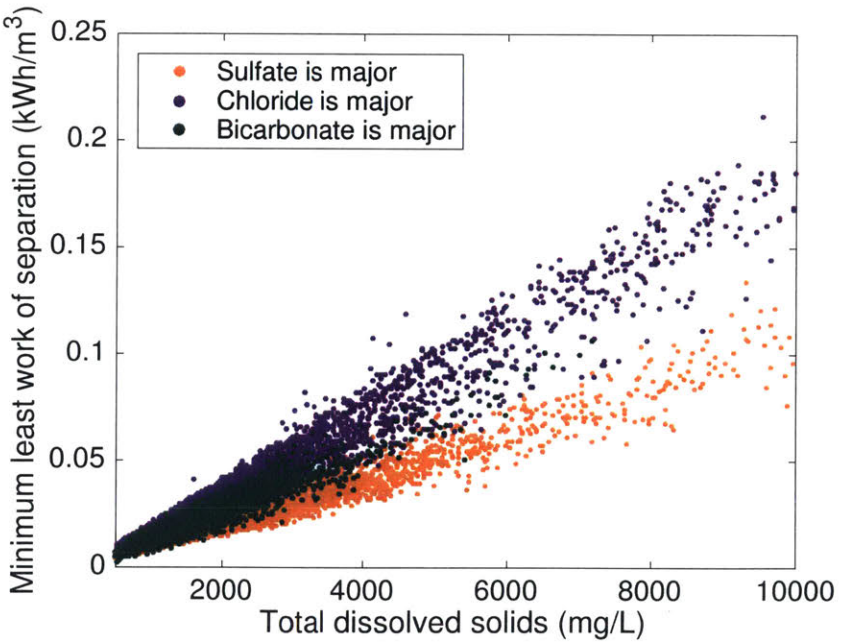


Figure G-2: Minimum least work of separation as a function of TDS for 28,000 BGW with complete composition data. Each dot corresponds to a BGW sample and is colored based on its major anion, defined in Eq. (G.1).

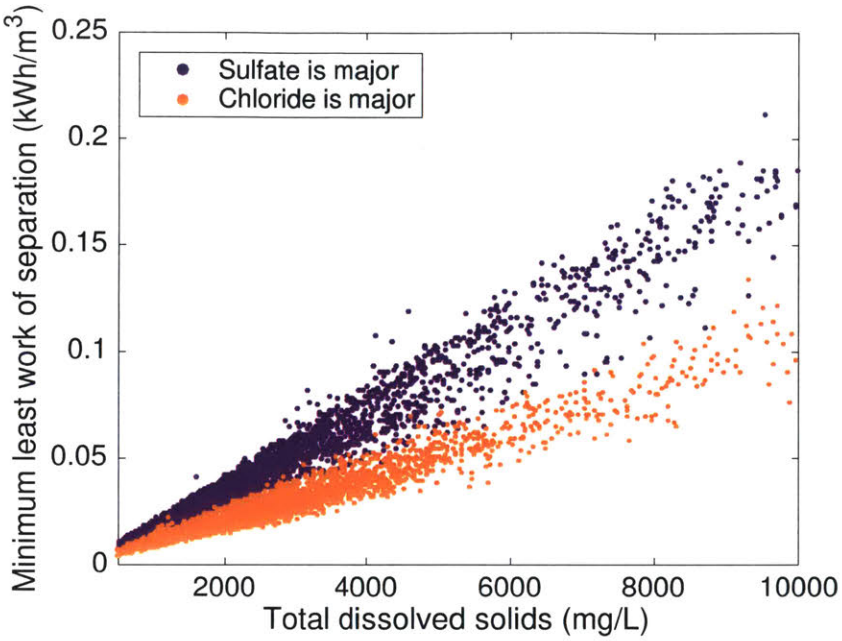


Figure G-3: Minimum least work of separation as a function of TDS for 28,000 BGW with complete composition data. Each dot corresponds to a BGW sample and is colored based on its major anion, defined in Eq. (G.1). Only chloride and sulfate are included in order to more clearly show tail formation in Fig. 4-5.

# Bibliography


[1] United Nations World Water Assesment Programme. *The United Nations World Water Development Report 2016: Water and Jobs.* Paris, France, 2016.

[2] M. A. Maupin, J. F. Kenny, S. S. Hutson, J. K. Lovelace, N. L. Barber, and K. S. Linsey. *Estimated use of water in the United States in 2010.* 2014.

[3] J. S. Stanton et al. *Brackish groundwater in the United States.* Reston, VA, 2017, p. 202.

[4] R. W. Miller. "The World's Water, 2000-2001: The Biennial Report on Freshwater Resources". *Electronic Green Journal* 1.16 (2002).

[5] P. McMahon, J. Böhlke, K. Dahm, D. Parkhurst, D. Anning, and J. Stanton. "Chemical Considerations for an Updated National Assessment of Brackish Groundwater Resources". *Groundwater* 54.4 (2016), pp. 464–475.

[6] A. Phocaides. *Handbook on Pressurized Irrigation Techniques.* 2nd ed. Rome, Italy: Food and Agriculture Organization of the United Nations, 2007.

[7] R. Ayers and D. Westcot. *Water quality for agriculture.* Food and Agriculture Organization of the United Nations, 1985.

[8] L. V. Wilcox. *Classification and use of irrigation waters.* Washington, DC, 1995.

[9] Environmental Protection Agency. *Edition of the Drinking Water Standards and Health Advisories.* Washington, DC, 2012.

[10] National Research Council. *Desalination: A national perspective.* Washington, D.C.: The National Academics Press, 2008, p. 316.

[11] M. Mickley. "US Municipal Desalination Plants: Number, Types, Locations, Sizes, and Concentrate Management Practices". *IDA Journal of Desalination and Water Reuse* 4.1 (2012), pp. 44–51.

[12] R. H. Stewart. *Introduction to Physical Oceanography.* Texas A & M University, 2008.

[13] W. H. Organization. *Desalination for safe water supply: guidance for the health and environmental aspects applicable to desalination.* Geneva, Switzerland, 2007.

[14] S. Qi and A. Harris. *Geochemical Database for the Brackish Groundwater Assessment of the United States.* 2017.

[15] Global Water Intelligence. *GWI DesalData.* Electronic. Oxford, England, 2016.

[16] F. J. Millero and A. Poisson. "International one-atmosphere equation of state of seawater". *Deep Sea Research Part A. Oceanographic Research Papers* 28.6 (1981), pp. 625 –629.

[17] W. Stumm and J. J. Morgan. *Aquatic Chemistry: Chemical Equilibria and Rates in Natural Waters.* 3rd ed. Vol. 126. New York: John Wiley Sons, Inc., 1996.

[18] P. Debye and E. Hückel. "The theory of electrolytes I. Freezing point depression and related phenomena". *Physikalische Zeitschrift* 24 (1923), pp. 185–206.

[19] K. S. Pitzer. *A thermodynamic model for aqueous solutions of liquid-like density.* 1987.

[20] K. S. Pitzer. "Thermodynamics of electrolytes. I. Theoretical basis and general equations". *The Journal of Physical Chemistry* 77.2 (1973), pp. 268–277.

[21] K. H. Mistry, R. K. McGovern, G. P. Thiel, E. K. Summers, S. M. Zubair, and J. H. Lienhard V. "Entropy generation analysis of desalination technologies". *Entropy* 13.10 (2011), pp. 1829–1864.

[22] K. H. Mistry, H. A. Hunter, and J. H. Lienhard V. "Effect of composition and nonideal solution behavior on desalination calculations for mixed electrolyte solutions with comparison to seawater". *Desalination* 318 (2013), pp. 34 –47.

[23] C. E. Harvie, N. Møller, and J. H. Weare. "The prediction of mineral solubilities in natural waters: The Na-K-Mg-Ca-H-Cl-SO4-OH-HCO3-CO3-CO2-H2O system to high ionic strengths at 25 C". *Geochimica et Cosmochimica Acta* 48.4 (1984), pp. 723–751.

[24] C. E. Harvie and J. H. Weare. "The prediction of mineral solubilities in natural waters: the Na-K-Mg-Ca-Cl-SO4-H2O system from zero to high concentration at 25 °C". *Geochimica et Cosmochimica Acta* 44.7 (1980), pp. 981–997.

[25] K. Heger, M. Uematsu, and E. U. Franck. "The Static Dielectric Constant of Water at High Pressures and Temperatures to 500 MPa and 550 °C". *Berichte der Bunsengesellschaft für physikalische Chemie* 84.8 (1980), pp. 758–762.

[26] H. T. Kim and W. J. Frederick Jr. "Evaluation of Pitzer ion interaction parameters of aqueous electrolytes at 25. degree. C. 1. Single salt parameters". *Journal of Chemical and Engineering Data* 33.2 (1988), pp. 177–184.

[27] J. F. Zemaitis Jr, D. M. Clark, M. Rafal, and N. C. Scrivner. *Handbook of aqueous electrolyte thermodynamics: Theory application.* John Wiley Sons, 2010.

[28] R. T. Pabalan and K. S. Pitzer. "Thermodynamics of concentrated electrolyte mixtures and the prediction of mineral solubilities to high temperatures for mixtures in the system Na-K-Mg-Cl-SO4-OH-H2O". *Geochimica et Cosmochimica Acta* 51.9 (1987), pp. 2429 –2443.

[29] F. J. Millero and D. Pierrot. "A Chemical Equilibrium Model for Natural Waters". *Aquatic Geochemistry* 4.1 (1998), pp. 153–199.

[30] L. F. Silvester and K. S. Pitzer. "Thermodynamics of electrolytes. X. Enthalpy and the effect of temperature on the activity coefficients". *Journal of Solution Chemistry* 7.5 (1978), pp. 327–337.

[31] L. F. Greenlee, D. F. Lawler, B. D. Freeman, B. Marrot, and P. Moulin. "Reverse osmosis desalination: Water sources, technology, and today's challenges". *Water Research* 43.9 (2009), pp. 2317 –2348.

[32] F. Gassert, M. Landis, M. Luck, P. Reig, and T. Shiao. "Aqueduct Global Maps 2.0" (2013).

[33] R. L. Miller, W. L. Bradford, and N. E. Peters. *Specific Conductance: Theoretical Considerations and Application to Analytical Quality Control.* Denver, CO, 1988.

[34] P. Atkins and L. Jones. *Chemical Principles: The Quest for Insight.* Ed. by W. H. Freeman. 5th ed. New York, 2010.

[35] R. A. Robinson and R. H. Stokes. *Electrolyte solutions.* 2nd ed. Courier Corporation, 2002.

[36] Y. Roy, M. H. Sharqawy, and J. H. Lienhard V. "Modeling of flat-sheet and spiral-wound filtration configurations and its application in seawater nanofiltration". *Journal of Membrane Science* 493 (2015), pp. 360 –372.

[37] California Water Science Center. *California Drought.* 2017.

[38] J.-P. Nicot and B. R. Scanlon. "Water Use for Shale-Gas Production in Texas, U.S." *Enivronmental Sicence and Technology* 46.6 (2012), pp. 3580–3586.

[39] K. G. Nayar, N. C. Wright, G. P. Thiel, A. Winter V, and J. H. Lienhard V. "Energy requirements of alternative technologies for desalinating groundwater for irrigation". *IDA World Congress.* San Diego, CA, 2015.

[40] G. P. Thiel and J. H. Lienhard V. "Treating produced water from hydraulic fracturing: Composition effects on scale formation and desalination system selection". *Desalination* 346 (2014), pp. 54 –69.